both infections and chronic GVHD, with cGVHD at a median follow up of 40 months from transplantation (RIC, 39 vs. CIC, 45 months). The median onset of cGVHD was 112 days (RIC, 100 vs. CIC, 109 days), and 47 patients (RIC, $n = 26$; CIC, $n = 21$) developed progressive-type cGVHD at a median follow up of 32 months from diagnosis of cGVHD (RIC, 39 vs. CIC, 45 months). The severity of the Karnofsky performance status (KPS) score was significantly greater in the RIC group ($P = 0.045$).

Infectious complications

A total of 134 infectious episodes occurred in 83 patients (RIC, 51 vs. CIC, 32; $P = 0.73$), as shown in Table 3. Of these, 28 patients (RIC, 18 vs. CIC 10; $P = 0.83$) developed bacteremia, the causative organisms (43 positive cultures) of which are summarized in Table 4. Gram-positive bacteremia (27 positive cultures) was more common than gram-negative bacteremia (16 positive cultures). The bacteremia was caused by 2, 3, and 4 types of organisms in 4, 4, and 1 patient, respectively. The incidence of bacteremia was significantly higher in patients with the following factors: cGVHD including progressive types ($n = 15$, $P = 0.0027$), a KPS score ≥ 2 ($n = 11$, $P = 0.0062$) and a gastrointestinal (GI) score ≥ 2 ($n = 13$, $P < 0.0001$); PSL dose ≥ 1 mg/kg at the time of diagnosis ($n = 9$, $P = 0.00090$) and for the initial treatment of cGVHD ($n = 11$, $P = 0.0050$). CVC-related infections ($n = 11$) were caused by *Staphylococcus epidermidis* ($n = 4$), *Staphylococcus* species ($n = 2$), *Stenotrophomonas maltophilia* ($n = 2$), *Acinetobacter iwoffii* ($n = 1$), *Corynebacterium* species ($n = 1$), or methicillin-resistant *Staphylococcus aureus* (MRSA, $n = 1$). The incidence of CVC-related infections was significantly higher in patients with PSL dose ≥ 1 mg/kg at the time of diagnosis of cGVHD ($n = 4$, $P = 0.026$). Bacterial pneumonia was observed in 4 patients, and the isolated organisms were as follows: *Pseudomonas aeruginosa* ($n = 1$), *Hemophilus influenzae* ($n = 1$), *S. epidermidis* ($n = 1$), and *Staphylococcus* species ($n = 1$). The incidence of bacterial pneumonia ($n = 4$) was significantly higher in patients with PSL dose ≥ 1 mg/kg at the time of diagnosis ($n = 3$, $P = 0.0051$) and for the initial treatment of cGVHD ($n = 3$, $P = 0.021$). Invasive aspergillosis (IA) and *Candida* infections developed in 7 and 3 patients, respectively. All patients with IA had been given ≥ 0.5 mg of PSL/kg at the time of diagnosis of cGVHD. The incidence

Infectious complications associated with cGVHD

	Total (median onset, range, days)	RIC	CIC	*P*
Bacterial infections				
Bacteremia	28 (175, 104–1629)	18 (5)[1]	10 (2)	0.83
CVC-related	11 (123, 101–1774)	5 (0)	6 (0)	0.33
Pneumonia	4 (311, 101–1045)	3 (2)	1 (1)	0.99
Others[2]	16 (302, 102–1065)	7 (4)	9 (2)	0.11
Fungal infections				
Candida infection	3 (128, 101–358)	1 (0)	2 (0)	0.56
Invasive aspergillosis	7 (181, 112–1232)	6 (0)	1 (0)	0.26
Viral infections				
Adenoviral hemorrhagic cystitis	8 (192, 111–538)	5 (0)	3 (0)	0.99
CMV colitis	1 (343)	0 (0)	1 (0)	0.37
Cutaneous VZV	18 (502, 106–1684)	12 (0)	6 (0)	0.80
Influenza	4 (483, 355–898)	1 (0)	3 (0)	0.15
Others[3]	2 (133, 103–164)	1 (0)	1 (0)	0.99
CMV antigenemia	15 (140, 104–448)	11 (0)	4 (0)	0.42
Pneumoniae of unknown origin	32 (283, 101–1735)	18 (4)	14 (4)	0.41

[1]Number of infectious episodes (number of deaths) is shown.
[2]Others = sepsis of unknown origin (4 episodes), dermatitis (3), hemorrhagic cystitis (2), otitis media (2), meningitis (2), cholecystitis (1), pseudomembranous enterocolitis (1), and urinary tract infection (1).
[3]Others = herpes simplex viral esophagitis (1 episode) and meningitis (1).
cGVHD, chronic graft-versus-host disease; RIC, reduced-intensity regimen; CIC, conventional-intensity regimen; CVC, central venous catheter; CMV, cytomegalovirus; VZV, varicella zoster virus.

Table 3

Bacteremia associated with cGVHD

	RIC ($n = 18$)	CIC ($n = 10$)
Gram-positive organisms	16[1]	11
Staphylococcus epidermidis	7	2
Streptococcus species	2	3
Enterococcus species	3	0
Staphylococcus species	0	3
Bacillus species	0	1
Corynebacterium species	1	0
MRSA	0	1
Gram-positive cocci	3	1
Gram-negative organisms	10	6
Bacteroides species	3	2
Pseudomonas aeruginosa	2	2
Klebsiella species	2	0
Enterobacter species	0	1
Escherichia coli	0	1
Gram-negative rods	3	0

[1]Number of positive cultures.
cGVHD, chronic graft-versus-host disease; RIC, reduced-intensity regimen; CIC, conventional-intensity regimen; MRSA, methicillin-resistant *Staphylococcus aureus*.

Table 4

of IA was significantly higher in patients with cGVHD including a GI score ≥ 2 ($n = 4$, $P = 0.015$), PSL dose ≥ 1 mg/kg at the time of diagnosis ($n = 4$, $P = 0.0037$), and for the initial treatment of cGVHD ($n = 7$, $P < 0.0001$). Eighteen patients developed cutaneous varicella zoster virus (VZV); all responded promptly to acyclovir. Eight patients developed adenoviral hemorrhagic cystitis (HC); 2 of these 8 patients developed continuously complicated lethal bacteremia. The incidence of adenoviral HC was significantly higher in patients with cGVHD including a KPS score ≥ 2 ($n = 5$, $P = 0.0071$) and a GI score ≥ 2 ($n = 4$, $P = 0.026$); PSL dose ≥ 1 mg/kg at the time of diagnosis ($n = 4$, $P = 0.0069$); and for the initial treatment of cGVHD ($n = 5$, $P = 0.0060$). *De novo* CMV antigenemia before or after development of cGVHD was observed in 62 and 15 patients, respectively. Sixteen and 8 patients, respectively, died of bacterial infections and pneumoniae of unknown origin.

Discussion

In the present retrospective analysis, 57% (83/145) of patients with cGVHD developed infections, with a mortality rate of 27% (22/83). Although the limitations of this study were the retrospective study design and the differences in baseline characteristics in both the RIC and CIC groups, these results illustrate the importance of establishing more effective management of infectious complications associated with cGVHD, which are predictive of poor outcome for both RIC and CIC regimens.

In patients with cGVHD, the major source of bacteremia was heterogeneous, gram-positive organisms such as *S. epidermidis* and *Streptococcus* species, which were more common than gram-negative organisms, and bacteremia caused by *Pseudomonas aeruginosa*, including multidrug-resistant *P. aeruginosa*, occurred only in patients with cGVHD involving a GI tract score ≥ 2. Additionally, *Streptococcus pneumonia* sepsis was a risk factor for non-relapse mortality, as reported previously (4), and pneumococcal vaccination of transplant recipients was found to be relatively ineffective in the presence of cGVHD. In other studies with RIC regimens, the incidence of bacteremia appeared to be significantly lower than in the present study, but this may a result of the shorter follow-up periods in those studies (14, 15). Moreover, 29% (7/24) of the present patients with cGVHD involving a GI tract score ≥ 2 had received ≥ 2 mg of PSL/kg before developing cGVHD, and all 7 of these patients developed bacteremia. Although 50% (14/28) of patients with bacteremia received antibiotic

drugs and all 14 of these patients received intravenous immunoglobulin to maintain IgG levels at >400 mg/dL for prophylaxis of encapsulated bacteria and *Pneumocystis*, these results suggest that patients with cGVHD having a GI tract score ≥ 2, especially after high-dose PSL, are more likely to develop bacteremia than patients with cGVHD not having a GI tract score ≥ 2. This was probably due to colonization of the GI tract resulting from translocation into the bloodstream or disruption of the ecologic GI equilibrium involving GI bacterial overgrowth (e.g., use of antibiotic decontamination), increased permeability of the GI mucosal barrier (e.g., GVHD-induced mucosal damage), or deficiencies in the host immune defenses (e.g., use of immunosuppressive drugs). Thus, a review of strategies for prevention of bacteremia may lead to improvement of patient outcomes after allogeneic HSCT. That is, in patients with cGVHD having a GI tract score ≥ 2, restrictions on the use of broad-spectrum antibiotics may help reduce GI bacterial overgrowth, including overgrowth by antibiotic-resistant organisms, resulting from failure of the GI barrier. In contrast, we recognize the difficulty in identifying bacteremia using culturing blood. Our patients were immunocompromised hosts who presented with undifferentiated fever; therefore, blood culture results were often delayed well into the course of empirical therapy. There is a need to develop suitable strategies for screening of bacteremia associated with cGVHD in patients who receive allogeneic HSCT with either RIC or CIC regimens.

Most of the present patients with cGVHD who developed *Candida* infection or IA received ≥ 0.5 mg of PSL/kg before developing cGVHD and the incidence of IA was significantly higher in patients with cGVHD having a GI score ≥ 2, especially after high-dose PSL. The number of patients with fungal infections was small, but high-dose PSL may be effective for improving the prophylaxis for such infections. Furthermore, the duration of prophylaxis still remains unclear as randomized clinical trials have yet to be conducted.

All the present patients with adenoviral HC developed grades II–IV acute GVHD and received PSL for GVHD therapy, which differs considerably from what has been reported previously(16). The incidence of adenoviral HC was significantly higher in patients with cGVHD having a KPS score ≥ 2, a GI score ≥ 2, and high-dose PSL at the time of diagnosis and for the initial treatment of cGVHD. Although the present study was limited in its ability to detect risk factors for adenoviral HC, because of low patient numbers and lack of prospective investigation of viral infection, the present results suggest that patients who receive high-dose PSL before and after developing cGVHD should be frequently checked for abdominal and urinary symptoms, and that urinary tests should be regularly performed during ongoing use of immunosuppressive drugs. In addition, we identified only 1 patient with cGVHD who suffered from CMV colitis, indicating that it is useful to monitor and treat CMV antigenemia intensively in patients receiving immunosuppressive drugs, especially before development of cGVHD. In contrast, 12% of the present patients with cGVHD developed cutaneous VZV with a median onset of 502 days (range, 106–1684), despite low-dose acyclovir prophylaxis during at least the first year after allogeneic HSCT. Nonetheless, there were no cases of breakthrough VZV infection. This suggests that low-dose acyclovir prophylaxis effectively prevented breakthrough VZV infection, but that reestablishment of antiviral therapy was needed to protect against cutaneous VZV in patients with cGVHD.

In summary, the present data indicate that infections associated with cGVHD, especially after high-dose PSL, are predictive of poor outcome, whether RIC or CIC is used. Accordingly, there is a need for clinical trials to develop new strategies for screening and prevention of infections associated with cGVHD in patients who receive allogeneic HSCT with either RIC or CIC regimens.

References

1. Perez-Simon JA, Diez-Campelo M, Martino R, et al. Influence of the intensity of the conditioning regimen on the characteristics of acute and chronic graft-versus-host disease after allogeneic transplantation. Br J Haematol 2005; 130: 394–403.
2. Hori A, Kami M, Kim SW, et al. Development of early neutropenic fever, with or without bacterial infection, is still a significant complication after reduced-intensity stem cell transplantation. Biol Blood Marrow Transplant 2004; 10: 65–72.
3. Kojima R, Tateishi U, Kami M, et al. Chest computed tomography of late invasive aspergillosis after allogeneic hematopoietic stem cell transplantation. Biol Blood Marrow Transplant 2005; 11: 506–511.
4. Kulkarni S, Powles R, Treleaven J, et al. Chronic graft versus host disease is associated with long-term risk for pneumococcal infections in recipients of bone marrow transplants. Blood 2000; 95: 3683–3686.
5. Dykewicz CA. Summary of the guidelines for preventing opportunistic infections among hematopoietic stem cell transplant recipients. Clin Infect Dis 2001; 33: 139–144.
6. Sepkowitz KA. Opportunistic infections in patients with and patients without acquired immunodeficiency syndrome. Clin Infect Dis 2002; 34: 1098–1107.
7. Atsuta Y, Suzuki R, Yamamoto K, et al. Risk and prognostic factors for Japanese patients with chronic graft-versus-host disease after bone marrow transplantation. Bone Marrow Transplant 2006; 37: 289–296.
8. Sorror ML, Maris MB, Storb R, et al. Hematopoietic cell transplantation (HCT)-specific comorbidity index: a new tool for risk assessment before allogeneic HCT. Blood 2005; 106: 2912–2929.
9. Kanda Y, Mineishi S, Saito T, et al. Long-term low-dose acyclovir against varicella-zoster virus reactivation after allogeneic hematopoietic stem cell transplantation. Bone Marrow Transplant 2001; 28: 689–692.

10. Doney KC, Weiden PL, Storb R, Thomas ED. Treatment of graft-versus-host disease in human allogeneic marrow graft recipients: a randomized trial comparing antithymocyte globulin and corticosteroids. Am J Hematol 1981; 11: 1–9.
11. Shulman HM, Sullivan KM, Weiden PL, et al. Chronic graft-versus-host syndrome in man. A long-term clinicopathologic study of 20 Seattle patients. Am J Med 1980; 69: 204–217.
12. Filipovich AH, Weisdorf D, Pavletic S, et al. National Institutes of Health consensus development project on criteria for clinical trials in chronic graft-versus-host disease: I. Diagnosis and staging working group report. Biol Blood Marrow Transplant 2005; 11: 945–956.
13. Ascioglu S, Rex JH, De Pauw B, et al. Defining opportunistic invasive fungal infections in immunocompromised patients with cancer and haematopoietic stem cell transplants: an international consensus. Clin Infect Dis 2002; 34: 7–14.
14. Junghanss C, Marr KA, Carter RA, et al. Incidence and outcome of bacterial and fungal infections following nonmyeloablative compared with myeloablative allogeneic hematopoietic stem cell transplantation: a matched control study. Biol Blood Marrow Transplant 2002; 8: 512–520.
15. Busca A, Locatelli F, Barbui A, et al. Infectious complications following nonmyeloablative allogeneic hematopoietic stem cell transplantation. Transpl Infect Dis 2003; 5: 132–139.
16. El-Zimaity M, Saliba R, Chan K, et al. Hemorrhagic cystitis after allogeneic hematopoietic stem cell transplantation: donor type matters. Blood 2004; 103: 4674–4680.

Oncogene (2007), 1–7

www.nature.com/onc

ORIGINAL ARTICLE

Virus-mediated oncolysis induces danger signal and stimulates cytotoxic T-lymphocyte activity via proteasome activator upregulation

Y Endo[1,2], R Sakai[1,2], M Ouchi[3], H Onimatsu[3], M Hioki[1,2], S Kagawa[1,2], F Uno[1,2], Y Watanabe[3], Y Urata[3], N Tanaka[1] and T Fujiwara[1,2]

[1]Division of Surgical Oncology, Department of Surgery, Okayama University Graduate School of Medicine, Dentistry and Pharmaceutical Sciences, Okayama, Japan; [2]Center for Gene and Cell Therapy, Okayama University Hospital, Okayama, Japan and [3]Oncolys BioPharma Inc., Tokyo, Japan

Dendritic cells (DCs) are the most potent antigen-presenting cells and acquire cellular antigens and danger signals from dying cells to initiate antitumor immune responses via direct cell-to-cell interaction and cytokine production. The optimal forms of tumor cell death for priming DCs for the release of danger signals are not fully understood. OBP-301 (Telomelysin) is a telomerase-specific replication-competent adenovirus that induces selective E1 expression and exclusively kills human cancer cells. Here, we show that OBP-301 replication produced the endogenous danger signaling molecule, uric acid, in infected human tumor cells, which in turn stimulated DCs to produce interferon-γ (IFN-γ) and interleukin 12 (IL-12). Subsequently, IFN-γ release upregulated the endogenous expression of the proteasome activator PA28 in tumor cells and resulted in the induction of cytotoxic T-lymphocytes. Our data suggest that virus-mediated oncolysis might be the effective stimulus for immature DCs to induce specific activity against human cancer cells.
Oncogene advance online publication, 5 November 2007; doi:10.1038/sj.onc.1210884

Keywords: adenovirus; telomerase; dendritic cell; uric acid; danger signal

Introduction

Dendritic cells (DCs) are the most important professional antigen-presenting cells and play a critical role in the induction of primary immune responses against tumor-associated antigens. Mature DCs express high levels of major histocompatibility complex (MHC) class I, II and co-stimulatory molecules such as CD80 and CD86, and secrete T-helper type-1 (Th1) cytokines such as interleukin (IL)-12 and interferon (IFN)-γ. DCs acquire endogenous maturation stimuli from dying cells as a danger signal when they capture cellular antigens. Lack of danger signals delays maturation of DCs and causes active suppression of DCs stimulatory capacity, leading to the induction of T-cell tolerance (Steinman *et al.*, 2000). Shi *et al.* (2003) have previously identified uric acid as a novel endogenous warning molecule capable of alerting the immune system within cell lysates. The uric acid activates DCs following relocation from the inside to the outside of injured cells and converts immunity from non-protective to protective. In fact, it has been reported that uric acid levels are elevated in tumors undergoing immune rejection and that the inhibition of uric acid production delays tumor regression (Hu *et al.*, 2004).

Viruses have evolved to infect, replicate in and kill human cells through diverse mechanisms such as direct cell death machinery and fairly brisk immune responses. We reported previously that telomerase-specific replication-competent adenovirus (Telomelysin, OBP-301), in which the human telomerase reverse transcriptase (hTERT) promoter element drives the expression of *E1A* and *E1B* genes linked with an internal ribosome entry site (IRES), induced selective E1 expression and efficiently killed human cancer cells, but not normal human fibroblasts (Kawashima *et al.*, 2004; Umeoka *et al.*, 2004; Taki *et al.*, 2005; Watanabe *et al.*, 2006). Although the precise molecular mechanism of OBP-301-induced cell death is still unclear, the process of oncolysis is morphologically distinct from apoptosis and necrosis. These findings led us to examine whether tumor cells killed by OBP-301 infection could stimulate DCs, thus enhancing the immune response.

In the present study, we compared three types of tumor preparations as a source of cell-derived antigen for the priming of DCs: virus-induced oncolysis, chemotherapeutic drug-induced apoptosis and necrosis by freeze/thaw. We also explored the cytokine signature and activating property of these cells for antitumor immune response against human cancer cells.

Results

We first examined whether OBP-301 infection affects the viability of human cancer cells using the XTT assay.

Correspondence: Dr T Fujiwara, Center for Gene and Cell Therapy, Okayama University Hospital, 2-5-1 Shikata-cho, Okayama 700-8558, Japan.
E-mail: toshi_f@md.okayama-u.ac.jp
Received 30 July 2007; revised 14 September 2007; accepted 17 September 2007

OBP-301 infection induced death of human cancer cell lines (H1299 human lung cancer and SW620 human colorectal cancer cells) in a dose-dependent manner (Figure 1). Although autophagy, or type II programmed cell death, partially involved in the cell death machinery triggered by OBP-301 infection, oncolytic cells are distinct from apoptotic cells (Supplementary Figure 1).

We next examined whether OBP-301 infection modulated intracellular concentrations of uric acid that might act as a danger signal in tumor cells. Uric acid levels increased in H1299 cells following OBP-301 infection in a time-dependent fashion, although docetaxel slightly upregulated the uric acid concentration 72 h after treatment (Figure 2a). Thus, tumor cells undergoing oncolysis can produce significantly greater amounts of uric acid when compared with apoptotic tumor cells. The uric acid elevation pattern of OBP-301-infected cells almost paralleled that of cells infected with Onyx-015, an E1B 55 kDa-deleted adenovirus engineered to selectively replicate in and lyse p53-deficient cancer cells, and wild-type adenovirus type 5 (Figure 2b), indicating a general effect of adenovirus infection in the regulation of intracellular uric acid levels.

Uric acid is produced during the catabolism of purines and is the end product of this process. Adenoviral replication facilitates the purine catabolism to stimulate the synthesis of progeny DNA, which in turn may increase intracellular uric acid levels by the purine degradation process. In fact, OBP-301 infection significantly increased the amount of uric acid in the cells, whereas replication-deficient dl312 infection had no apparent effect on the levels of uric acid. OBP-301-induced elevation of uric acid levels could be inhibited in the presence of cidofovir (CDV), an acyclic nucleoside phosphonate having potent broad-spectrum anti-DNA virus activity (Figure 2c). CDV has been approved for the treatment of many types of viruses including cytomegalovirus and adenovirus (Lenaerts and Naesens, 2006). We confirmed that CDV at 100 μM could significantly inhibited replication of OBP-301 in H1299 cells by the real-time quantitative PCR analysis (Supplementary Figure 2). Moreover, as OBP-301 replication was attenuated in telomerase-negative cells, the levels of uric acid could not be altered in normal human lung fibroblasts (NHLF) after OBP-301 infection (Figure 2d). These results suggest that viral replication is required to produce uric acid in infected cells.

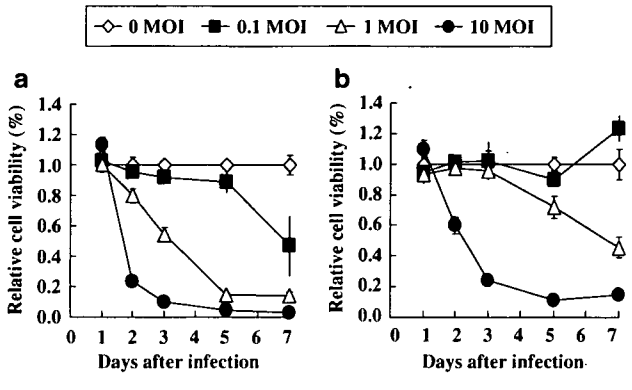

Figure 1 *In vitro* cytopathic effects of OBP-301 on human cancer cells. H1299 human non-small cell lung cancer (**a**) and SW620 human colorectal cancer cells (**b**) were infected with OBP-301 at indicated multiplicity of infection (MOI) values, and surviving cells were quantitated over 7 days by XTT assay. The cell viability of mock-treated cells on day 1 was considered 1.0, and the relative cell viability was calculated. Each data represent the mean ± standard deviation (s.d.) of triplicate experiments.

Xanthine oxidoreductase (XOR) is a member of the molybdoflavoenzyme family that catalyses the formation of uric acid from xanthine and hypoxanthine (Glantzounis *et al.*, 2005). A strand-specific reverse transcriptase PCR assay demonstrated that XOR mRNA expression gradually decreased in OBP-301-infected cells presumably due to the negative feedback of increased uric acid levels, whereas docetaxel-treated cells yielded consistent bands of the XOR transcripts (Figure 2e). Thus, adenoviral replication could directly stimulate the catalytic DNA turnover, which enables cells to produce more uric acid.

We then examined the ability of OBP-301-infected cells to stimulate immature DCs *in vitro*. DCs generated from HLA-A24$^+$ healthy volunteers were co-cultured with HLA-matched H1299 cells (HLA-A32/A24) treated with OBP-301 or docetaxel for 72 h, or freeze thawed. The production of Th1 cytokines such as IFN-γ and IL-12 in the supernatants was then explored by enzyme-linked immunosorbent assay (ELISA) analysis 48 h after the co-culture. DCs incubated with OBP-301-infected cells secreted large amounts of IFN-γ and IL-12, whereas stimulation with docetaxel-treated apoptotic cells induced their secretion at low levels (Figure 3a). The level of cytokine production from DCs incubated with freeze-thawed necrotic cells was similar to that of untreated immature DCs. Moreover, we confirmed that addition of OBP-301 alone without target tumor cells did not affect the cytokine secretion of DCs into the supernatant, indicating that infection of OBP-301 itself had no apparent effect on DCs. Thus, DCs stimulated with oncolytic tumor cells preferentially secrete high-level Th1 cytokines. Flow cytometry demonstrated that the increase in the expression of CD83, which is expressed on mature DCs, was slightly higher on DCs incubated with oncolytic cells than those with apoptotic or necrotic cells, indicating that oncolytic tumor cells seems to have a positive influence on DC maturation (Supplementary Figure 3).

In the next step, we investigated the effects of oncolytic tumor cells on T-cell activation in the presence of DCs. H1299 cells were infected with OBP-301 over 72 h, and then co-incubated with HLA-matched HLA-A24$^+$ peripheral blood mononuclear cells (PBMCs) for another 48 h in mixed lymphocyte tumor culture (MLTC). In other tests, H1299 cells were exposed to docetaxel for 72 h or freeze thawed, and then co-cultured with PBMCs. We examined the secretion of IFN-γ and IL-12 into the supernatants after MLTC for 7 days. Stimulation with OBP-301-infected cells induced the secretion of high levels of IFN-γ and IL-12 into MLTC supernatants, which was significantly higher

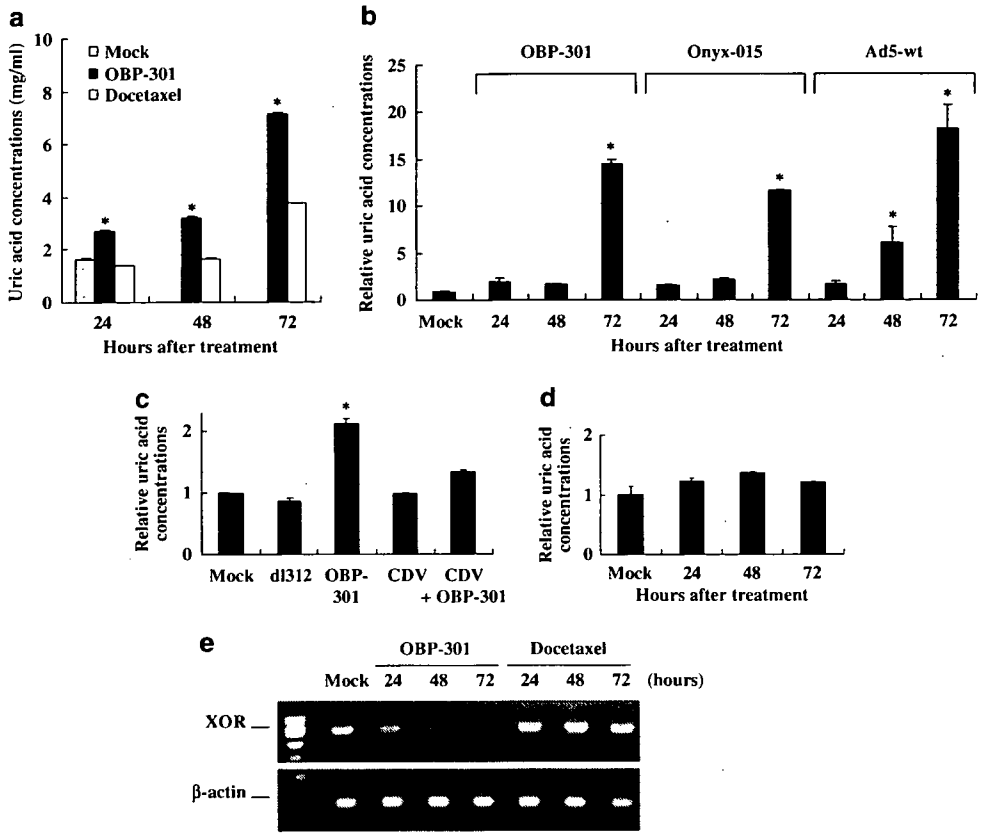

Figure 2 (a) Uric acid concentrations in H1299 cells treated with OBP-301 or docetaxel. H1299 cells were infected with 1.0 MOI of OBP-301 or treated with 10 nM of docetaxel for indicated time periods, and uric acid concentrations were determined enzymatically in the cell homogenates. Single asterisk indicates $P < 0.01$, significantly different from docetaxel-treated cells. (**b**) Uric acid levels in H1299 cells treated with OBP-301, Onyx-015 or wild-type adenovirus. H1299 cells were harvested at indicated time points over 72 h after infection with 10 MOI of viruses, and subjected to the measurement of uric acid concentrations. The levels of uric acid concentration are defined as the fold-increase for each sample relative to that of mock-treated cells (mock equals 1). Single asterisk indicates $P < 0.01$, significantly different from mock-treated cells. (**c**) Uric acid concentrations in H1299 cells infected with 1.0 MOI of OBP-301 or replication-deficient dl312 adenovirus were measured 24 h after infection. Uric acid production was also assessed in H1299 cells infected with 1.0 MOI of OBP-301 in the presence of 100 μM of anti-virus agent cidofovir (CDV). H1299 cells treated with 100 μM of CDV were subjected to the assay as a control. All uric acid levels are normalized to that of mock-treated cells (mock equals 1). (**d**) Uric acid levels in NHLF infected with OBP-301. NHLF cells were infected with 1.0 MOI of OBP-301 for indicated time periods, and uric acid concentrations were measured. The uric acid levels are normalized to that of mock-treated cells. (**e**) Detection of xanthine oxidoreductase (XOR) mRNA expression in OBP-301-infected H1299 cells by RT–PCR analysis. Cells were infected with 1.0 MOI of OBP-301 or treated with 10 nM of docetaxel, and then collected at the indicated time points. First-strand DNA generated from RNA was amplified using either the primers specific for XOR sequence or the primers that recognize β-actin sequences as an internal control.

than that with docetaxel-treated or freeze-thawed H1299 cells (Figure 3b). Thus, oncolytic tumor cells can accelerate the cleavage of tumor antigen peptides that can be associated with MHC class I molecules via IFN-γ secretion by immune cells.

Stimulation of cells with IFN-γ is known to induce the expression of PA28, a proteasome activator that accelerates the *in vitro* processing of MHC class I ligands from their polypeptide precursors (Sun *et al*., 2002). We investigated whether PA28 expression was upregulated in H1299 cells by adding the supernatants of co-cultures of PBMCs and OBP-301-infected H1299 cells. Western blot analysis for PA28 demonstrated that, following heat inactivation of residual OBP-301, MLTC supernatants with oncolytic tumor cells induced a strong endogenous PA28 expression in H1299 cells. In contrast, exposure to the supernatants of PBMCs alone, PBMCs with untreated H1299 cells, and PBMCs with oncolytic tumor cells without heat inactivation resulted in no apparent changes in the expression levels of PA28 (Figure 4).

Finally, the cytotoxic T-lymphocyte (CTL) response against human cancer cells was assessed by a standard 6-h ^{51}Cr release assay after a 7-day MLTC using various forms of H1299 cells. The lytic activity of CTLs induced by apoptotic or necrotic H1299 cells was comparable with that of human lymphokine-activated killer (LAK) cells; CTLs stimulated with oncolytic H1299 cells, however, more efficiently killed target H1299 cells (Figure 5). In contrast, LAK cells effectively lysed SW620 cells, whereas these cells were minimally killed by CTLs stimulated with apoptotic, necrotic or oncolytic H1299 cells. Furthermore, HLA-unmatched, HLA-A26/A30$^+$ A549 human lung cancer cells were not sensitive to oncolytic tumor cell-induced cytotoxicity (data not shown), suggesting that effector cells stimulated with

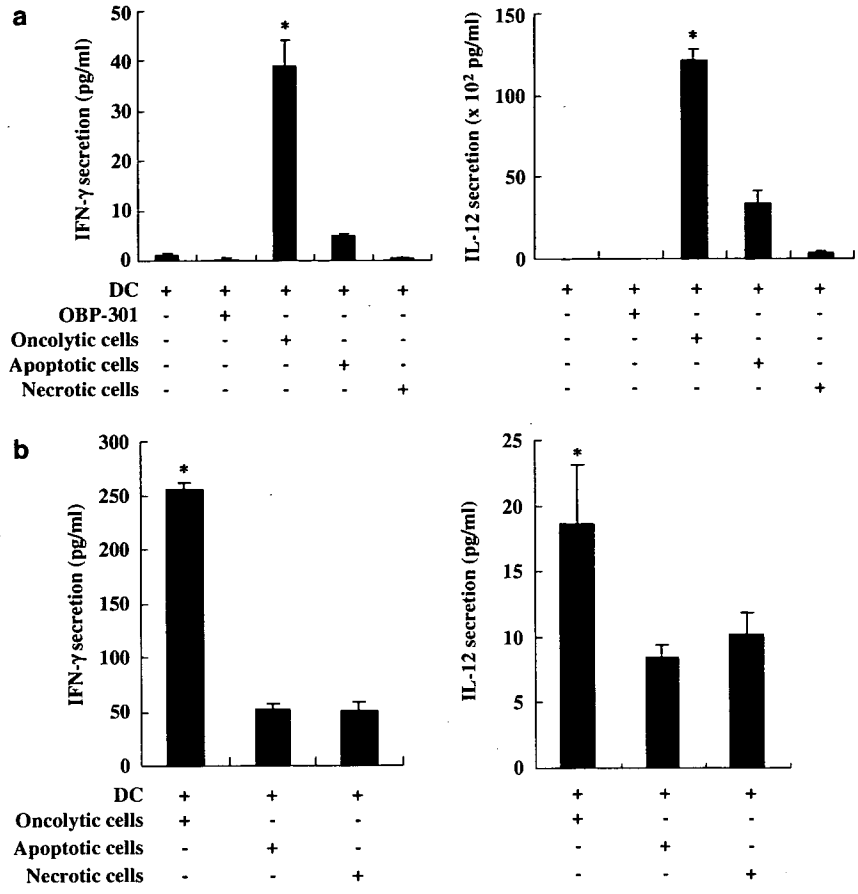

Figure 3 (**a**) Secretion of Th1-type cytokines by oncolytic, apoptotic or necrotic tumor cells. H1299 cells were treated with 1.0 MOI of OBP-301 or 50 nM of docetaxel for 72 h, or freeze thawed, and then co-cultured with immature dendritic cells (DCs) obtained from monocytes for additional 48 h. The culture supernatants were harvested and tested by ELISA for interferon (IFN)-γ (left) and interleukin (IL)-12 (right) concentrations. As a control, the supernatants of immature DCs alone or with OBP-301 at an MOI of 1.0 were also examined. Data are mean ± s.d. of triplicate experiments. Single asterisk indicates $P<0.01$, significantly different from other groups. (**b**) Tumor-specific CTL induction in MTLC with oncolytic, apoptotic or necrotic tumor cells. IFN-γ (left) and IL-12 (right) concentrations in the supernatants of MLTC analysed by ELISA. H1299 cells were treated with 1.0 MOI of OBP-301 or 50 nM of docetaxel for 72 h, or freeze thawed, and then co-cultured with PBMCs obtained from HLA-A24$^+$ healthy volunteers for 48 h in MLTC. Data are mean ± s.d. of triplicate experiments. Single asterisk indicates $P<0.01$, significantly different from other groups.

OBP-301-infected tumor cells exhibit MHC class I-restricted reactivity.

Discussion

In the present study, our goal was to determine whether oncolytic virus is effective not only as a direct cytotoxic drug but also as an immunostimulatory agent that could induce specific CTL for the remaining antigen-bearing tumor cells. Several groups have debated whether necrotic or apoptotic cells can stimulate DCs to cross-present cell-derived peptides, with subsequent enhancement of tumor immunogenicity. Furthermore, it has been reported recently that the immunogenicity of tumors is not regulated by signals associated with apoptotic or necrotic cell death, but is an intrinsic feature of the tumor itself (Bartholomae *et al*., 2004). Our data indicate that viral oncolysis could efficiently load tumor antigen on DCs, and then generate CTL response as judged from the production of cytokines. Moreover, the CTL activity against untreated tumor cells suggests that CTLs are specific to tumor antigens, but not to adenovirus proteins.

DCs are known to ingest dying tumor cells and initiate tumor-specific responses when associated with appropriate danger signals, which are endogenous activation signals liberated by dying cells. Recent studies have shown that some intrinsic biochemical factors, such as uric acid, bradykinin and heat shock protein (HSP110) act as danger signals through their interaction with DCs, and influence the subsequent immune response (Aliberti *et al*., 2003; Shi *et al*., 2003; Manjili *et al*., 2005). Large amounts of uric acid can be produced following tissue injury *in vivo*, and activate the immune response against injured cells and dying tissues. We found that OBP-301 infection increased intracellular uric acid levels in human tumor cells compared with apoptosis- or necrosis-inducing stimuli, suggesting that viral replication itself can enhance tumorigenicity.

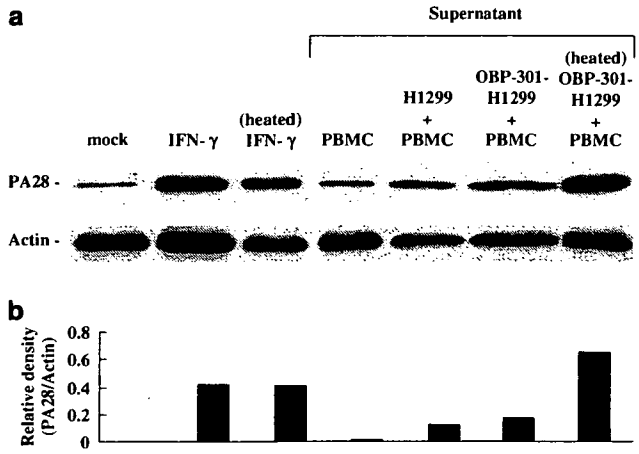

Figure 4 (**a**) Western blot analysis of PA28 in H1299 cells exposed to the supernatants of MLTC. peripheral blood mononuclear cells (PBMCs) were incubated with mock, untreated H1299 cells or H1299 cells treated with 10 MOI of OBP-301 for 72 h in MLTC, and the supernatants were harvested 48 h after the co-culture. H1299 cells were further incubated with the supernatants for 72 h with or without heat inactivation of residual virus (56 °C, 10 min). H1299 cells were also incubated with 5 ng ml^{-1} of interferon (IFN)-γ with or without heating for 72 h. Equivalent amounts of protein obtained from whole cell lysates were loaded in each lane, probed with anti-PA28 antibody and then visualized by using an ECL detection system. Equal loading of samples was confirmed by stripping each blot and reprobing with anti-actin antiserum. (**b**) PA28 protein expression was quantified by densitometric scanning using NIH Image software and normalization by dividing the actin signal.

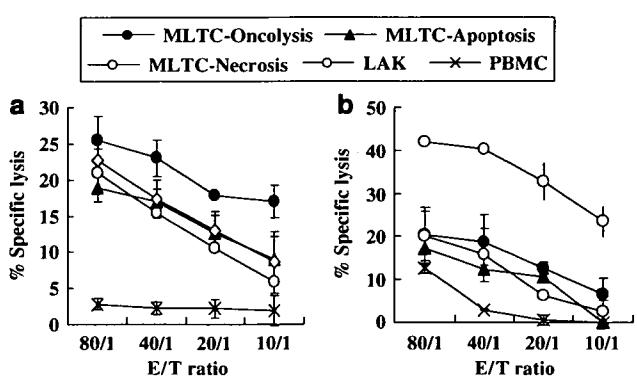

Figure 5 Cytolytic reactivity against H1299 (**a**) and SW620 (**b**) human cancer cells was assessed after 7-day mixed lymphocyte tumor culture (MLTC) with oncolytic, apoptotic or necrotic H1299 cells treated the same as above by 6-h standard ^{51}Cr-release assay. Lymphokine-activated killer (LAK) cells were generated from peripheral blood mononuclear cells (PBMCs) in the presence of interleukin (IL)-2 (100 U ml^{-1}) for 3 days. The CTLs were compared with LAK cells and untreated PBMCs, which served as positive and negative controls, respectively. Data represent the mean ± s.d. of three wells at four different effector-to-target (E/T) ratios.

Viral oncolysis increases the immunogenicity of tumor cells presumably by the release of proinflammatory cytokines (Lindenmann and Klein, 1967). We showed that OBP-301-infected oncolytic tumor cells efficiently stimulated immature DCs to produce greater amounts of IFN-γ and IL-12 than apoptotic and necrotic cells, and that such stimulation led to DC maturation. Viral infection itself has been reported to activate DCs to secrete pro- or anti-inflammatory cytokines, which can drive DCs to undergo the maturation process (Ho *et al*., 2001); the observation that OBP-301 alone had no effect on cytokine production by DCs, however, indicates that OBP-301 itself may be less infective or stimulatory to DCs. The result is consistent with our finding that OBP-301 attenuated replication as well as cytotoxicity in human normal cells.

It will be of interest to more mechanistically define why viral oncolysis efficiently induces CTL activity against tumor cells. We hypothesized that viral replication itself or the released cytokines by immune cells positively influences tumor cell immunogenicity. The IFN-γ-inducible proteasome modulator complex PA28 participates in the generation of antigenic peptides required for MHC class I antigen presentation (Sijts *et al*., 2002). As expected, the supernatants of MLTC with OBP-301-infected tumor cells, in which IFN-γ secretion was detected, induced a strong expression of endogenous PA28. Thus, oncolytic tumor cells can accelerate the cleavage of tumor antigen peptides that can be associated with MHC class I molecules via IFN-γ secretion by immune cells. In fact, it has been reported that restoration of PA28 expression in PA28-deficient melanoma cells rescues the melanoma antigen epitope presentation (Sun *et al*., 2002); our preliminary experiments however demonstrated that human tumor cells transfected with PA28α expression vector were less sensitive to tumor-specific CTLs (data not shown). These observations suggest that antigen peptide production alone does not seem sufficient to enhance tumor immunogenicity.

In conclusion, we provide for the first time evidence that oncolytic virus replication induces tumor-specific immune responses by stimulating uric acid production as a danger signal as well as accelerating tumor antigen cleavage by IFN-γ-inducible PA28 expression. Since the induction of systemic immunity has rarely been observed in clinical trials with other conditionally replication-competent viruses, more *in vivo* experiments are clearly required to support the induction of antitumor immunity by OBP-301 treatment. Our data, however, suggest that the antitumor effect of OBP-301 might be potentially both direct and indirect as well as systemic rather than local.

Materials and methods

Cell lines and reagents

The human non-small lung cancer cell lines H1299 (HLA-A32/A24) and the human colorectal carcinoma cell lines SW620 (HLA-A02/A24) were maintained *in vitro* in RPMI 1640 supplemented with 10% fetal calf serum, 100 U ml^{-1} penicillin and 100 mg ml^{-1} streptomycin. Recombinant human cytokines granulocyte/macrophage colony-stimulating factor (GM-CSF), IL-4, TNF-α and IL-7 were purchased from Genzyme

Techne (Minneapolis, MN, USA), IFN-γ from Peprotech (Rocky Hill, NJ, USA) and IL-2 from Roche (Mannheim, Germany). [^{51}Cr] sodium chromate was obtained from NEN Life Science Products (Boston, MA, USA). Docetaxel (taxotere) was kindly provided by Aventis Pharma (Tokyo, Japan).

Adenovirus
The recombinant replication-selective, tumor-specific adenovirus vector OBP-301 (Telomelysin), in which the hTERT promoter element drives the expression of *E1A* and *E1B* genes linked with an IRES, was constructed and characterized previously (Kawashima *et al*., 2004; Umeoka *et al*., 2004; Taki *et al*., 2005; Watanabe *et al*., 2006). Onyx-015 (dl1520) is an E1B 55 kDa-deleted adenovirus engineered to selectively replicate in and lyse p53-deficient cancer cells, and kindly provided by Dr Frank McCormick (UCSF Comprehensive Cancer Center and Cancer Research Institute). The E1A-deleted adenovirus vector lacking a cDNA insert (dl312) was also used as a control vector. The viruses were purified by $CsCl_2$ step gradient ultracentrifugation followed by $CsCl_2$ linear gradient ultracentrifugation.

Cell viability assay
XTT assay was performed to measure cell viability. Briefly, cells were plated on 96-well plates at 5×10^3 per well 24 h before treatment and then infected with OBP-301 or exposed to docetaxel. Cell viability was determined at the times indicated by using a Cell Proliferation Kit II (Roche Molecular Biochemicals) according to the protocol provided by the manufacturer.

Reverse transcription (RT)–PCR
Total RNA was isolated from mock-, OBP-301- and docetaxel-treated cells using RNAzol (Cinna/BioTecx, Friendswood, TX, USA) in a single-step phenol-extraction method and used as templates. Reverse transcription was performed at 22 °C for 10 min and then 42 °C for 20 min using 1.0 μg of RNA per reaction to ensure that the amount of amplified DNA was proportional to that of specific mRNA in the original sample. PCR was performed with specific primers in volumes of 50-μl according to the s protocol provided by the manufacturer (PCR kit; Perkin-Elmer/Cetus, Norwalk, CT, USA). The specific primers used for XOR were 5′-GCG AAG GAT AAG GTT ACT TGT-3′ (forward) and 5′-CTC CAG GTA GAA GTG CTC TTG-3′ (reverse); and for β-actin were 5′-ATG GTG GGA ATG GGT CAG AAG-3′ (forward) and 5′-GCA GCT CAT TGT AGA AGG-3′ (reverse). The reaction conditions were denaturing at 94 °C for 2 min followed by 30 cycles consisting of denaturing at 94 °C (30 s), annealing at 65 °C (15 s) and extension at 72 °C (10 s) using a thermal cycler (Perkin-Elmer, Foster City, CA, USA). The reactions were completed by a final 2-min extension at 72 °C. The PCR products were resolved on 1% agarose gels and visualized by SYBR Gold Nucleic Acid Gel Stain (Molecular Probes Inc., Eugene, OR, USA).

Preparation of tumor cells
For induction of oncolysis, tumor cells were infected with OBP-301 at a multiplicity of infection (MOI) of 1–10, and then collected 24–72 h after infection. Apoptotic tumor cells were obtained after 24–72-h exposure to 50–100 nM of docetaxel. For induction of necrosis, tumor cells suspended in phosphate-buffered saline (PBS) were subjected to rapid four freeze/thaw cycles using a 60 °C water bath and liquid nitrogen.

Measurement of uric acid concentration
Cultured cells were harvested after treatment and rinsed three times with PBS. These cells were resuspended in lysis buffer at a density of 200×10^6 cells per 100 μl. The buffer contained 10 mM Tris–HCl (pH 7.5), 150 nM NaCl, 50 mM NaF, 1 mM ethylenediaminetetraacetic acid (EDTA), 0.5 mM Na_3VO_4, 10% glycerol, 0.5% NP-40 and 0.1 mM phenylmethylsulfonyl fluoride (PMSF). After 10-s homogenization, the resulting extracts were kept on ice for 30 min and then were centrifuged for 15 min at 2000 *g*. The supernatants from treated tumor cells were assayed for uric acid using Uric Acid C test (Wako, Osaka, Japan).

Preparation of DCs
Peripheral blood samples were obtained from normal HLA-A24 positive healthy volunteers and PBMC were isolated by sedimentation over Ficoll-Hypaque. They were subsequently allowed to adhere in culture flasks for 1 h at 37 °C at a density of 4.0×10^7 cells per plate. Non-adherent cells in the plate were removed and the remaining (adherent) cells were cultured for 7 days in AIM-V (Gibco, Rockville, MD, USA) containing 2% heated-inactivated autologous serum supplemented with GM-CSF (50 ng ml^{-1}) and IL-4 (50 ng ml^{-1}).

Cytokine production assay
DCs were co-cultured with treated tumor cells at a ratio of 3:1 (DC/tumor cell) in a culture medium containing GM-CSF (50 ng ml^{-1}) and IL-4 (50 ng ml^{-1}). After 24-h incubation, the supernatant was collected and stored at −80 °C until the assay. The concentrations of IFN-γ and IL-12 (p40 and p70) were measured with appropriate ELISA kits (BioSource, Camarillo, CA, USA).

MLTC and CTL assay
PBMCs were co-cultured with treated tumor cells at a ratio of 20:1 in the presence of IL-2 (Roche) (10 U ml^{-1}) and IL-7 (Genzyme Techne) (5 ng ml^{-1}) for 7 days. Cultured cells were then used as effector cells in a standard 4 h-^{51}Cr release assay and the percentage of lysed cells was calculated. Percent specific lysis = ((experimental cpm − spontaneous cpm)/(maximal cpm − spontaneous cpm) × 100). Supernatants from MLTC performed as above were also assayed for IFN-γ and IL-12 by ELISA assays (BioSource).

Western blot analysis
The primary antibodies against proteasome activator PA28 (ZMD353; Invitrogen, Carlsbad, CA, USA), actin (AC-40; Sigma Chemical Co., St. Louis, MO, USA) and peroxidase-linked secondary antibody (Amersham, Arlington Heights, IL, USA) were used. Cells were washed twice in cold PBS and collected, then lysed in lysis buffer (10 mM Tris (pH 7.5), 150 mM NaCl, 50 mM NaF, 1 mM EDTA, 10% glycerol and 0.5% NP40) containing proteinase inhibitors (0.1 mM PMSF and 0.5 mM Na_3VO_4). After 20 min on ice, the lysates were spun at 14 000 rpm in a microcentrifuge at 4 °C for 10 min. The supernatants were used as whole cell extracts. Protein concentration was determined using the Bio-Rad protein determination method (Bio-Rad, Richmond, CA, USA). Equal amounts (50 μg) of proteins were boiled for 5 min and electrophoresed under reducing conditions on 6–12.5% (w/v) polyacrylamide gels. Proteins were electrophoretically transferred to a Hybond-polyvinylidene difluoride transfer membranes (Amersham Life Science, Buckinghamshire, UK), and incubated with the primary antibody, followed by peroxidase-linked secondary antibody. An Amersham ECL

chemiluminescent western system (Amersham) was used to detect secondary probes.

Statistical analysis

Data are expressed as mean ± s.d. The Student's *t*-test was used to compare differences. Statistical significance was defined when P was <0.05.

Acknowledgements

We thank Drs Tamotsu Yoshimori and Frank McCormick for providing pLC3-GFP plasmid and Onyx-015, respectively.

The study was supported by Grants-in-Aid from the Ministry of Education, Science and Culture, Japan; and Grants from the Ministry of Health and Welfare, Japan.

References

Aliberti J, Viola JP, Vieira-de-Abreu A, Bozza PT, Sher A, Scharfstein J. (2003). Bradykinin induces IL-12 production by dendritic cells: a danger signal that drives Th1 polarization. *J Immunol* **170**: 5349–5353.

Bartholomae WC, Rininsland FH, Eisenberg JC, Boehm BO, Lehmann PV, Tary-Lehmann M. (2004). T cell immunity induced by live, necrotic, and apoptotic tumor cells. *J Immunol* **173**: 1012–1022.

Glantzounis GK, Tsimoyiannis EC, Kappas AM, Galaris DA. (2005). Uric acid and oxidative stress. *Curr Pharm Des* **11**: 4145–4151.

Ho LJ, Wang JJ, Shaio MF, Kao CL, Chang DM, Han SW *et al.* (2001). Infection of human dendritic cells by dengue virus causes cell maturation and cytokine production. *J Immunol* **166**: 1499–1506.

Hu DE, Moore AM, Thomsen LL, Brindle KM. (2004). Uric acid promotes tumor immune rejection. *Cancer Res* **64**: 5059–5062.

Kawashima T, Kagawa S, Kobayashi N, Shirakiya Y, Umeoka T, Teraishi F *et al.* (2004). Telomerase-specific replication-selective virotherapy for human cancer. *Clin Cancer Res* **10**: 285–292.

Lenaerts L, Naesens L. (2006). Antiviral therapy for adenovirus infections. *Antiviral Res* **71**: 172–180.

Lindenmann J, Klein PA. (1967). Viral oncolysis: increased immunogenicity of host cell antigen associated with influenza virus. *J Exp Med* **126**: 93–108.

Manjili MH, Park J, Facciponte JG, Subjeck JR. (2005). HSP110 induces 'danger signals' upon interaction with antigen presenting cells and mouse mammary carcinoma. *Immunobiology* **210**: 295–303.

Shi Y, Evans JE, Rock KL. (2003). Molecular identification of a danger signal that alerts the immune system to dying cells. *Nature* **425**: 516–521.

Sijts A, Sun Y, Janek K, Kral S, Paschen A, Schadendorf D *et al.* (2002). The role of the proteasome activator PA28 in MHC class I antigen processing. *Mol Immunol* **39**: 165–169.

Steinman RM, Turley S, Mellman I, Inaba K. (2000). The induction of tolerance by dendritic cells that have captured apoptotic cells. *J Exp Med* **191**: 411–416.

Sun Y, Sijts AJ, Song M, Janek K, Nussbaum AK, Kral S *et al.* (2002). Expression of the proteasome activator PA28 rescues the presentation of a cytotoxic T lymphocyte epitope on melanoma cells. *Cancer Res* **62**: 2875–2882.

Taki M, Kagawa S, Nishizaki M, Mizuguchi H, Hayakawa T, Kyo S *et al.* (2005). Enhanced oncolysis by a tropism-modified telomerase-specific replication-selective adenoviral agent OBP-405 ('Telomelysin-RGD'). *Oncogene* **24**: 3130–3140.

Umeoka T, Kawashima T, Kagawa S, Teraishi F, Taki M, Nishizaki M *et al.* (2004). Visualization of intrathoracically disseminated solid tumors in mice with optical imaging by telomerase-specific amplification of a transferred green fluorescent protein gene. *Cancer Res* **64**: 6259–6265.

Watanabe T, Hioki M, Fujiwara T, Nishizaki M, Kagawa S, Taki M *et al.* (2006). Histone deacetylase inhibitor FR901228 enhances the antitumor effect of telomerase-specific replication-selective adenoviral agent OBP-301 in human lung cancer cells. *Exp Cell Res* **312**: 256–265.

Supplementary Information accompanies the paper on the Oncogene website (http://www.nature.com/onc).

Establishment of biological and pharmacokinetic assays of telomerase-specific replication-selective adenovirus

Yuuri Hashimoto,[1] Yuichi Watanabe,[1] Yoshiko Shirakiya,[1] Futoshi Uno,[2] Shunsuke Kagawa,[2] Hitoshi Kawamura,[1] Katsuyuki Nagai,[1] Noriaki Tanaka,[3] Horomi Kumon,[2] Yasuo Urata[1] and Toshiyoshi Fujiwara[2,4]

[1]Oncolys BioPharma, 3-16-33 Roppongi, Minato-ku, Tokyo 106-0031; [2]Center for Gene and Cell Therapy, Okayama University Hospital, 2-5-1 Shikata-cho, Okayama 700-8558; [3]Division of Surgical Oncology, Department of Surgery, Okayama University Graduate School of Medicine and Dentistry, 2-5-1 Shikata-cho, Okayama 700-8558, Japan

(Received June 25, 2007/Revised September 11, 2007/Accepted October 4, 2007/Online publication January 14, 2008)

The use of replication-selective tumor-specific viruses represents a novel approach for the treatment of neoplastic disease. We constructed an attenuated adenovirus, telomerase-specific replication-selective adenovirus (TRAD), in which the human telomerase reverse transcriptase promoter element drives the expression of the *E1A* and *E1B* genes linked with an internal ribosome entry site (IRES). Forty-eight hours after TRAD infection at a multiplicity of infection of 1.0, the cell viability of H1299 human lung cancer cells was consistently less than 50% and therefore this procedure could be used as a potency assay to assess the biological activity of TRAD. We also established a quantitative real-time polymerase chain reaction (PCR) analysis with consensus primers for either the adenovirus E1A or IRES sequence. The linear ranges of quantitation with E1A and IRES primers were 10^3–10^8 and 10^2–10^8 plaque-forming units/mL in the plasma, respectively. The PCR analysis demonstrated that the levels of *E1A* in normal tissues were more than 10^3 lower than in the tumors of A549 human lung tumor xenografts in *nu/nu* mice at 28 days after intratumoral injection. Our results suggest that the cell-killing assay against H1299 cells and real-time PCR can be used to assess the biological activity and biodistribution of TRAD in clinical trials. (*Cancer Sci* 2008; 99: 385–390)

The emerging fields of functional genomics and functional proteomics provide an expanding repertoire of clinically applicable targeted therapeutics.[1] Replication-selective oncolytic viruses provide a new platform for treatment of a variety of human cancers.[2,3] Promising clinical trials have shown the antitumor potency and safety of mutant or genetically modified adenoviruses.[4,5] We constructed previously an adenovirus vector, TRAD, in which the hTERT promoter element drives the expression of the *E1A* and *E1B* genes linked with an IRES. We showed that TRAD caused efficient selective killing of human cancer cells, but not normal cells.[6] Many studies have demonstrated that the majority of malignant tumors express telomerase activity,[7] suggesting that TRAD can potentially kill most human cancer cells.

TRAD can replicate and then lyse cancer cells, infect neighboring cancer cells, and subsequently induce oncolysis throughout the whole tumor mass *in vivo*. As preclinical models showed that TRAD could spread into the bloodstream, it is important to monitor carefully the amount of TRAD in the circulation after intratumoral injection of TRAD to avoid serious adverse events due to viremia. Although we used vector-specific primers that detected the p53 open reading frame–adenoviral DNA junction in a phase I clinical trial of a replication-deficient adenoviral vector expressing the wild-type *p53* gene (Advexin),[8] no appropriate method has been established to detect TRAD quantitatively. In addition, there is also a need for a procedure that can evaluate the biological activity of TRAD for clinical application.

In the present study, we characterized a potent antitumor viral agent, TRAD, to establish a biological assay and developed a single quantitative PCR method that can be used to assess the number of viral genomes present in the plasma as well as tissues.

Materials and Methods

Cells and culture conditions. H1299 (a human non-small-cell lung cancer cell line), H460 (a human large-cell lung cancer cell line), A549 (a human lung adenocarcinoma cell line), LNCap (a human metastatic prostate carcinoma cell line), MKN28 and MKN45 (human gastric adenocarcinoma cell lines), PC-3 (a human prostate adenocarcinoma cell line), SW620 (a human colorectal carcinoma cell line), and TE8 and T.Tn (human esophagus squamous carcinoma cell lines) were propagated to monolayer cultures in RPMI-1640 supplemented with 10% FBS, and 100 units/mL PG and 100 μg/mL SM. HeLa (a human cervical adenocarcinoma cell line), HepG2 (a human hepatocellular carcinoma cell line), Panc-1 (a human pancreatic epithelioid carcinoma cell line), and 293 (a transformed embryonic kidney cell line) were grown in DMEM containing high glucose (4.5 g/L) (high) with 10% FBS and PG/SM. HT-29 (a human colorectal adenocarcinoma cell line) was grown in McCoy's 5a with 10% FBS and PG/SM. MCF-7 (a human mammary gland adenocarcinoma cell line) was grown in Earle's Minimum Essential Medium with 10% FBS, PG/SM, and 2 mM L-glutamine. OST, SaOS2, and HOS (human osteosarcoma cell lines) were grown in DMEM (high) with 10% FBS and PG/SM. HSC-3 and HSC-4 (human tongue squamous carcinoma cell lines) were obtained from the Health Science Resources Bank (Osaka, Japan) and grown in DMEM (high) with 10% FBS and PG/SM. SCC-4 and SCC-9 (human tongue squamous carcinoma cell lines) were obtained from American Type Culture Collection (ATCC, Rockville, MD, USA) and grown in DMEM containing Nutrient Mixture (Ham's F-12) with 10% FBS, PG/SM, and 400 ng/mL hydrocortisone. U-2OS (a human osteosarcoma cell line) was obtained from ATCC and grown in McCoy's 5a with 10% FBS and PG/SM. NHLF was purchased from Takara Biomedicals (Kyoto, Japan) and cultured in the medium recommended by the manufacturer.

Recombinant adenoviruses. The recombinant replication-selective tumor-specific adenovirus vector TRAD was constructed and

[4]To whom correspondence should be addressed. E-mail: toshi_f@md.okayama-u.ac.jp

Abbreviations: ATCC, American Type Culture Collection; DMEM, Dulbecco's modified Eagle's medium; FBS, fetal bovine serum; hTERT, human telomerase reverse transcriptase; ID_{50}, the multiplicity of infection that causes 50% growth inhibition; IRES, internal ribosome entry site; NHLF, normal human lung fibroblasts; MOI, multiplicity of infection; PCR, polymerase chain reaction; PFU, plaque-forming units; PG, penicillin; SM, streptomycin; TRAD, telomerase-specific replication-selective adenovirus; XTT, sodium 3'-[1-(phenylaminocarbonyl)-3,4-tetrazolium]-bis(4-methoxy-6-nitro)benzene sulfonic acid hydrate.

doi: 10.1111/j.1349-7006.2007.00665.x

characterized as described previously.[6,9–11] The virus was purified by $CsCl_2$ step-gradient ultracentrifugation followed by $CsCl_2$ linear-gradient ultracentrifugation. The virus particle titer and infectious titer were determined spectrophotometrically and by plaque assay, respectively, in 293 cells.

Cell-viability assay. The XTT assay was carried out to measure cell viability. Cells were plated on 96-well plates at 1×10^3 cells/well 20 h before viral infection. HSC-4, SCC-4, and SCC-9 cells were then infected with TRAD at MOI of 0, 1, 10, and 50 PFU/cell. Other cell lines were infected with TRAD at MOI of 0, 0.1, 1, and 10 PFU/cell. Cell viability was determined at 1, 2, 3, and 5 days after virus infection using Cell Proliferation Kit II (Roche Molecular Biochemicals, Indianapolis, IN, USA) according to the protocol provided by the manufacturer. Using the cell viability data at 3 days after virus infection, we determined the TRAD ID_{50} of each cell line.

Cell-killing assay. H1299 cells were plated at 5×10^4 cells/well on 24-well plates and infected with TRAD at MOI of 0, 0.01, 0.1, 1, and 10 PFU/cell. Forty-eight hours later, the number of cells in each well was counted. Experiments were carried out in triplicate for each MOI, and cell viability was assessed by the trypan blue dye exclusion assay.

Quantitative real-time PCR assay. Viral DNA from serially diluted viral stocks and tumor cells infected with TRAD were extracted using QIAamp DNA Mini Kit (Qiagen, Valencia, CA, USA), and quantitative real-time PCR assay for either the *E1A* gene or the IRES sequence was carried out using a LightCycler instrument and a LightCycler DNA Master SYBR Green I kit (Roche Molecular Biochemicals). Typical amplification mixes (20 μL) contained 3 mM $MgCl_2$, 0.3 μM of each primer for IRES or 0.5 μM for *E1A*, and 2 μL of 10 × LightCycler FastStart DNA Master SYBR Green I. The sequences of the specific primers used in this experiment were: IRES, 5′-GAT TTT CCA CCA TAT TGC CG-3′ and 5′-TTC ACG ACA TTC AAC AGA CC-3′; E1A, 5′-CCT GTG TCT AGA GAA TGC AA-3′ and 5′-ACA GCT CAA GTC CAA AGG TT-3′. PCR amplifications were carried out in glass capillary tubes. PCR amplification for IRES began with a 10-min denaturation step at 95°C and then 40 cycles of denaturation at 95°C for 10 s, annealing at 60°C for 10 s, and extension at 72°C for 6 s. PCR amplification for *E1A* began with a 10-min denaturation step at 95°C and then 40 cycles of denaturation at 95°C for 10 s, annealing at 58°C for 15 s, and extension at 72°C for 8 s. Data analysis was carried out using LightCycler Software (Roche Molecular Biochemicals).

***In vivo* human tumor model.** A549 human lung cancer cells (5×10^6 cells/mouse) were injected subcutaneously into the flank of 7- to 9-week-old female BALB/c *nu/nμ* mice and permitted to grow to approximately 5–6 mm in diameter. At that stage, a 100-μL solution containing 1×10^8 PFU of TRAD was injected into the tumor. The tumors and organs were harvested 28 and 70 days later and DNA was extracted from each tissue. To compare viral replication in the tumor and other normal organs, quantitative real-time PCR for the *E1A* gene was carried out using a LightCycler instrument. The experimental protocol was approved by the Ethics Review Committee for Animal Experimentation of Okayama University School of Medicine.

Statistical analysis. All data were expressed as mean ± SD. Differences between groups were examined for statistical significance using Student's *t*-test. A *P*-value less than 0.05 denoted the presence of a statistically significant difference.

Results

***In vitro* cytopathic efficacy of TRAD in human cancer cell lines derived from different organs.** To determine whether TRAD infection induces broad-spectrum selective cell lysis, 23 tumor cell lines derived from 11 different organs (head and neck, lung, esophagus, stomach, colon, liver, pancreas, breast, prostate, uterus, and bone) were infected with TRAD at various MOI. Previous studies using a real-time reverse transcription-PCR method have demonstrated that these cell lines express detectable levels of hTERT mRNA.[6,9] Cytotoxicity was then assessed using the XTT cell-viability assay over 5 days after infection. As shown in Figure 1a, TRAD infection induced cell death in all cell lines except T.Tn esophageal cancer cells in a dose-dependent manner. Calculated ID_{50} values confirmed that all cell lines except T.Tn could be killed efficiently by TRAD at an MOI of less than 25 (Fig. 1b). These results suggest the broad-spectrum antitumor potency of TRAD.

Establishment of a standard assay to assess the biological activity of TRAD. H1299 human lung cancer cells and LNCap human prostate cancer cells were the most sensitive cell lines to TRAD-induced cell death (Fig. 1b). Accordingly, we used H1299 cells to evaluate the biological activity of TRAD. To test whether the selective replication of TRAD translates into selective oncolysis, we compared the cytopathic effects of TRAD in H1299 cells and NHLF at 5 days after infection. The dose–response curve of the relative cell viability in H1299 cells was shifted to the left compared to that in NHLF, suggesting that TRAD killed H1299 cells 10^2–10^3 more efficiently than NHLF (Fig. 2a).

We next determined the minimal dose of TRAD that could induce more than 50% of cell death in H1299 cells. As shown in Figure 2b, the cell viability of H1299 cells was less than 40% at 48 h after their infection with TRAD at a MOI of 1.0, but was 60% after infection with a MOI of 0.1. We also confirmed that H1299 cells at various passages (5th to 20th after purchase from ATCC) could be killed by TRAD in a similar fashion (data not shown). Therefore, TRAD could be considered biologically active, if TRAD at a MOI of 1 reduces the cell viability of H1299 cells by more than 50% at 48 h after infection. To estimate the utility of this assay, we examined the biological activity of heat-inactivated TRAD. Infection with intact TRAD at a MOI of 10 induced approximately 90% reduction in H1299 cell viability at 48 h after infection, whereas the antitumor activity was completely inhibited when it was preheated at 56°C for 5 or 10 min (Fig. 2c).

Development of quantitative PCR assay to detect copy numbers of TRAD. We used real-time PCR for quantitative detection of TRAD. Oligonucleotide primers were designed to achieve DNA amplification of the adenoviral E1A or IRES sequences in the TRAD genome (Fig. 3a). To generate accurate standard curves, TRAD at a known concentration was serially diluted and used as a template for real-time PCR analysis. Detection of IRES and E1A genome copies was achieved consistently and reproducibly by the PCR cycle values used. A linear relationship could be obtained between the number of cycles and the $\log_{10}$ dilution when 10^2–10^8 IRES copies and 10^3–10^8 E1A copies were assayed. Regression analysis of IRES and E1A curves resulted in very high correlation coefficients (0.99 and 1.00, respectively) for these concentration ranges (Fig. 3b). In addition, the dilution of TRAD virus in the plasma did not affect the sensitivity and dynamic ranges of quantification (Fig. 3b), suggesting that this method can be used to detect TRAD in the blood circulation.

***In vitro* quantification and replication monitoring of TRAD in infected human tumor and normal cells.** We next examined the replication ability of TRAD in different cell lines by measuring the relative amounts of IRES and E1A copy numbers. LNCap and NHLF cells were harvested at the indicated time points over 5 and 7 days, respectively, after infection with TRAD, and subjected to quantitative real-time PCR analysis using IRES and E1A primers. The ratios were normalized by dividing the value of cells obtained at 2 h after viral infection. As shown in Figure 4a, TRAD replicated 10^3–10^4 by 5 days after infection; its replication, however, was attenuated to less than 10^3 in normal NHLF cells. We previously reported that TRAD could replicate 10^5–10^6 by 3 days after infection in H1299 cells;[6,10] however, as

doi: 10.1111/j.1349-7006.2007.00665.x

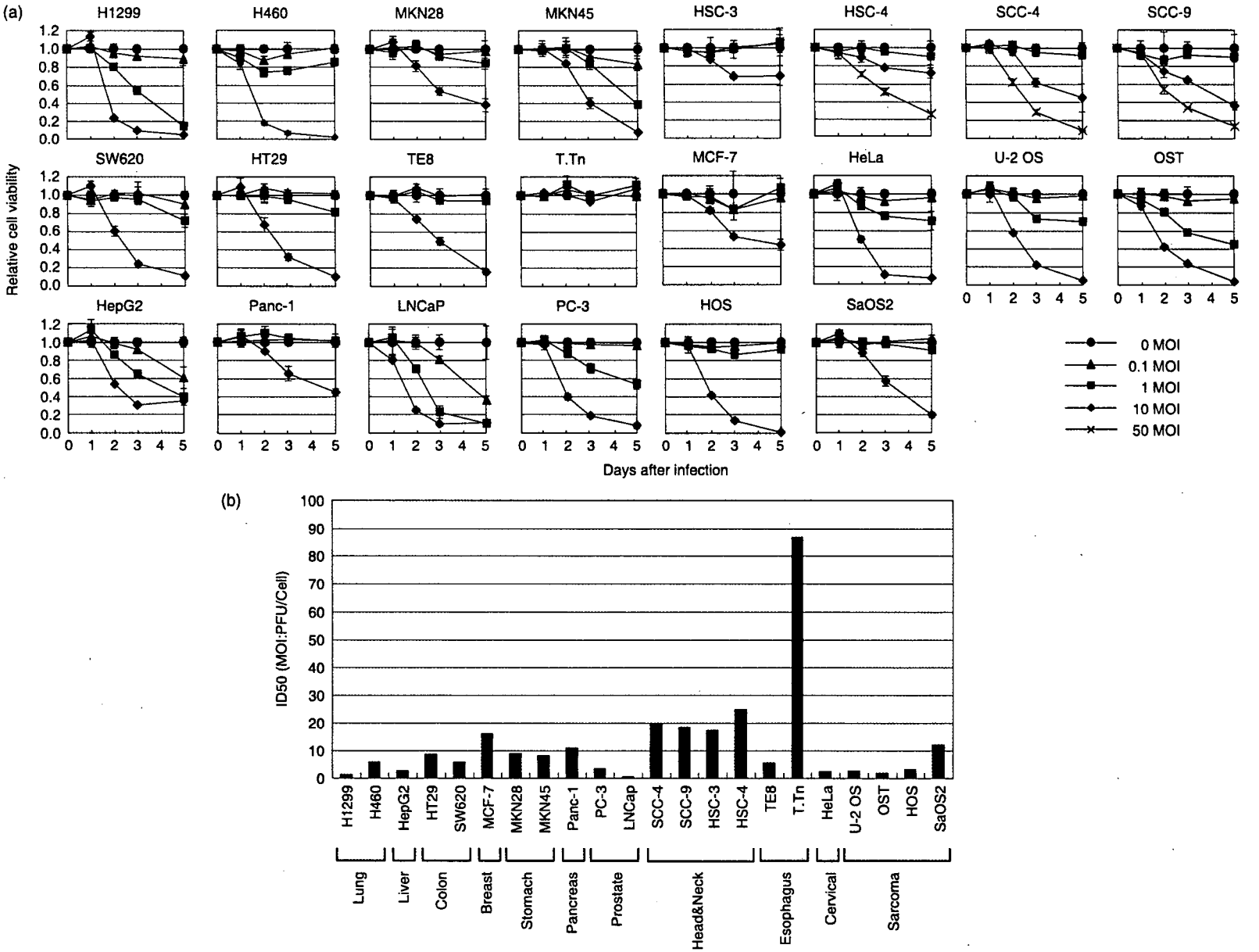

Fig. 1. Oncolytic effects of telomerase-specific replication-selective adenovirus (TRAD) *in vitro* on a variety of human cancer cell lines. (a) Cells were infected with TRAD at indicated multiplicity of infection (MOI) values, and surviving cells were quantitated over 5 days by XTT assay. Data are mean ± SD. (b) The 50% inhibiting doses of TRAD on cell viability at 3 days after infection were calculated and expressed as ID_{50} values. PFU, plaque-forming units; XXT, sodium 3′-[1-(phenylaminocarbonyl)-3,4-tetrazolium]-bis(4-methoxy-6-nitro)benzene sulfonic acid hydrate.

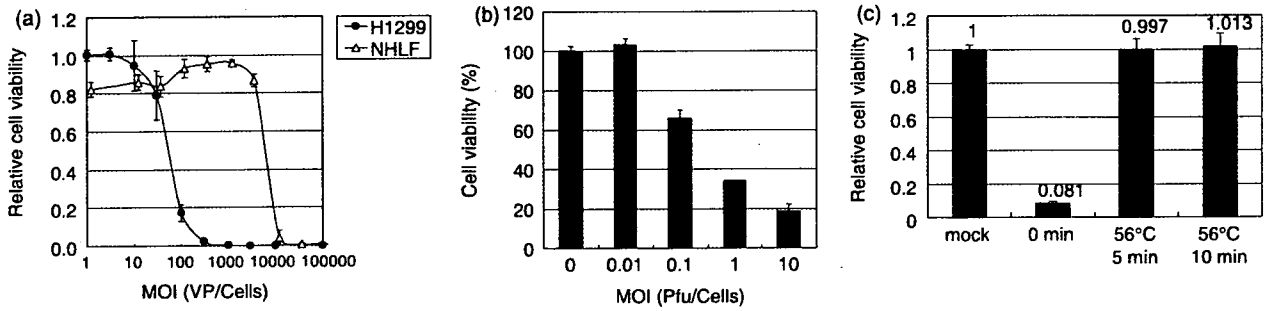

Fig. 2. Antitumor effects of telomerase-specific replication-selective adenovirus (TRAD) on H1299 non-small-cell lung cancer cells *in vitro*. (a) Effects of various concentrations of TRAD on H1299 cancer cells and normal human lung fibroblasts (NHLF) assessed at 5 days after treatment with XTT assay. Results are expressed as the percentage of untreated control. (b) H1299 cells were cultured as monolayers in triplicate in 24-well culture plates, infected with TRAD at the indicated multiplicities of infection (MOI), and assessed for cell viability 48 h after infection. Mock-infected cells were used as a control. (c) H1299 cells were plated on 96-well plates and infected with 10 MOI of TRAD heated at 56°C for 5 or 10 min, or non-treated TRAD. An XTT assay was carried out at 3 days after virus infection. Mock-infected cells were used as a control. Data represent the mean ± SD of triplicate experiments. PFU, plaque-forming units; XXT, sodium 3′-[1-(phenylaminocarbonyl)-3,4-tetrazolium]-bis(4-methoxy-6-nitro) benzene sulfonic acid hydrate; VP, virus particles.

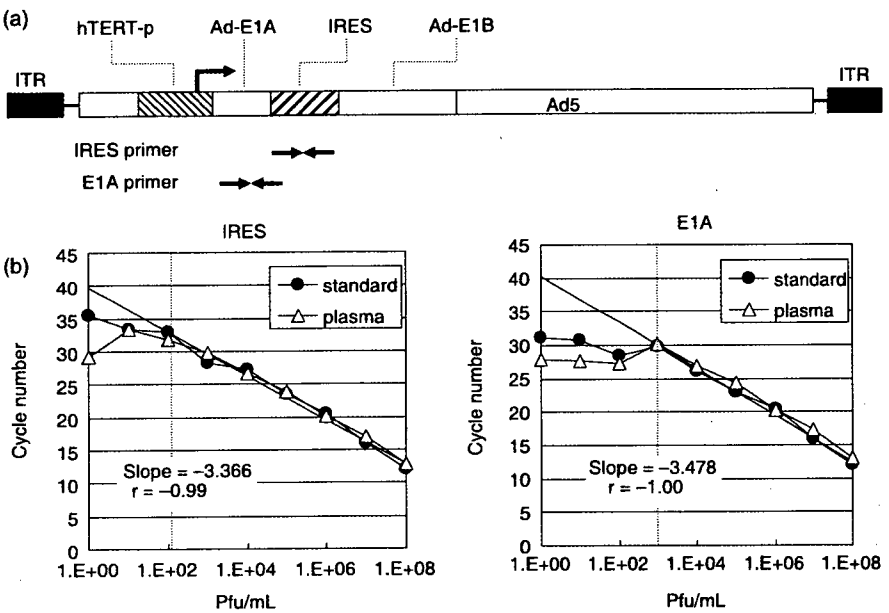

Fig. 3. Detection of normal human lung fibroblasts (TRAD) using quantitative polymerase chain reaction (PCR) assay. (a) Schematic diagram of the DNA structure of TRAD. TRAD contains the human telomerase reverse transcriptase (hTERT) promoter sequence inserted into the adenovirus genome to drive transcription of the *E1A* and *E1B* bicistronic cassette linked by the internal ribosome entry site (IRES) structure. Sites to which PCR primers (IRES and E1A) were targeted are indicated. Two primer pairs of IRES and E1A were designed to detect the TRAD genome. (b) Standard calibration curves of threshold cycle values and copy numbers are shown using serial dilution of TRAD virus stock. The coefficient of correlation (r^2) and slope are indicated for assays with IRES and E1A primers. ITR, inverted terminal repeats; PFU, plaque-forming units.

LNCap cells were more sensitive to TRAD-mediated cytotoxicity than H1299 cells (Fig. 1a), viral replication reached a plateau phase around 10^4 when LNCap cells started to die. Moreover, PCR targeting IRES and E1A showed similar replication profiles for TRAD in MCF-7 human breast cancer cells (Fig. 4b). To monitor the long-term viral replication, MCF-7 cells that were less sensitive to the cytopathic effect of the virus were used.

***In vivo* determination of TRAD genomes in tissue samples after intratumoral injection.** To evaluate selective replication of TRAD *in vivo*, we examined mouse tissues, including implanted tumors, for the presence of viral DNA by quantitative real-time PCR, following intratumoral viral injection. Mice with established subcutaneous A549 human lung tumor xenografts received a single intratumoral injection of 1×10^8 PFU of TRAD, and were killed 28 or 70 days after injection. To obtain the sufficient amounts of tumor tissues for analysis, we chose to use A549 cells. Our preliminary experiments demonstrated that intratumoral administration of TRAD suppressed tumor growth significantly compared with mock-treated tumors at 42 days after initiation of treatment ($P < 0.05$); however, the *in vivo* antitumor effect against A549 tumors was less than that against H1299 or LNCap tumors (data not shown). Although E1A DNA was detected in serum and some normal tissues examined (brain, heart, lung, ovary, liver, uterus, kidneys, bladder, colon, and axillary and mesenteric lymph nodes), tumors injected with TRAD contained at least 1000-fold more *E1A* copies (Fig. 5). These results suggest that quantitative real-time PCR allows detection and quantification of the number of TRAD genomes present in tissue samples after intratumoral injection of TRAD *in vivo*.

Discussion

Oncolytic viruses have been developed as anticancer agents based on the advantage of selective killing of tumor cells by controlled replication of the virus in the tumors, resulting in minimal undesired effects on normal cells.[2] Furthermore, amplified viruses can infect adjacent tumor cells as well as reach distant metastatic tumors through the blood circulation. Alhtough this might be a potential advantage of oncolytic viruses, systemic dissemination of large amounts of virus may induce virus-related symptoms including fever, diarrhea, pneumonia, and hepatitis, eventually leading to death. Therefore, virus shedding and distribution have to be evaluated by appropriate and suitable methods. In addition,

doi: 10.1111/j.1349-7006.2007.00665.x

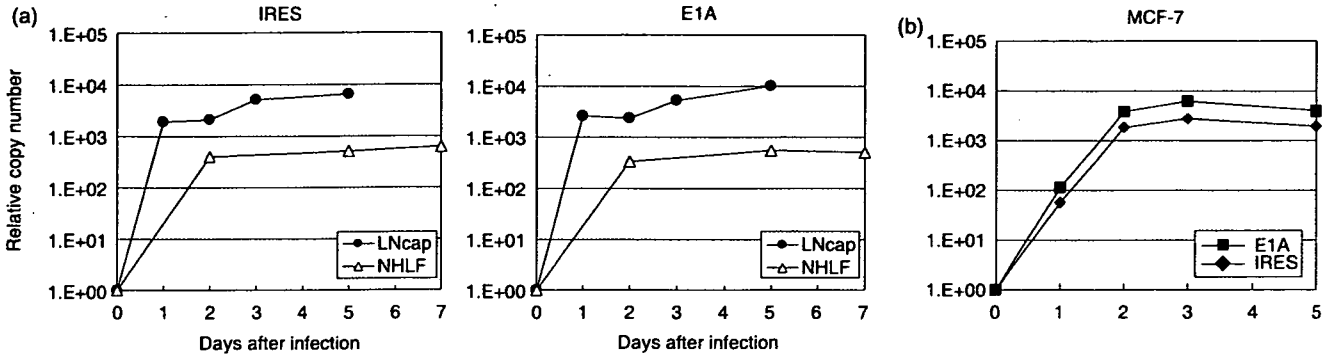

Fig. 4. Quantitative measurement of viral DNA replication in human cancer and normal cells *in vitro* by quantitative polymerase chain reaction (PCR) assay. (a) LNCap human prostate cancer cells and normal human lung fibroblast (NHLF) cells were infected with telomerase-specific replication-selective adenovirus (TRAD) at a multiplicity of infection (MOI) of 1 for 2 h. Following the removal of virus inoculum, cells were further incubated for the indicated periods of time, and then subjected to the real-time quantitative PCR assay. The amounts of viral internal ribosome entry site (IRES) and E1A copy number was defined as the fold increase for each sample relative to that at 2 h (2 h equals 1). (b) MCF-7 human breast cancer cells were infected with TRAD at a MOI of 1 and subjected to the PCR assay at the indicated time points. The relative TRAD DNA levels detected by IRES and E1A primers were plotted.

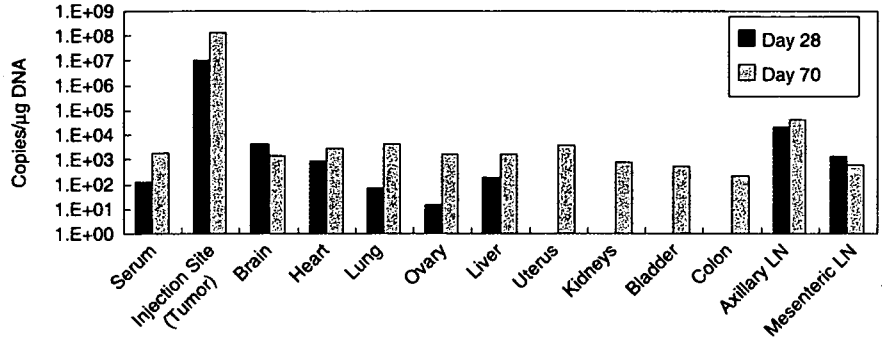

Fig. 5. Spread and replication of telomerase-specific replication-selective adenovirus (TRAD) following intratumoral administration in *nu/nμ* mice transplanted with A549 tumor cells. A549 tumor cells were injected subcutaneously into the right flank of mice at 5×10^6 cells/mouse. Mice received intratumoral injection of 1×10^8 plaque-forming units of TRAD when the tumor reached a size of approximately 5–6 mm in diameter. DNA was extracted from the subcutaneous tumor and various tissues of *nu/nμ* mice at 28 or 70 days after infection. Viral DNA was detected by quantitative polymerase chain reaction amplification of the adenoviral E1A sequence. The amounts of TRAD genome were defined as viral E1A copy number per μg DNA. LN, lymph nodes.

to avoid unexpected infectious disease due to viral overdose, we need assays that accurately detect the biological activity of viruses. In the present study, for clinical trials of TRAD, we developed an assay designed to estimate the biological activity of TRAD and to detect the copy number of TRAD in the plasma as well as tissues.

Although telomerase-specific TRAD exhibited a broad cytopathic effect against human cancer cell lines of different tissue origins, a human non-small-cell lung cancer cell line, H1299, was chosen for the biological assay of TRAD. H1299 was one of the most sensitive cell lines to TRAD-mediated cell death (ID_{50} = 0.94 MOI) and could be killed efficiently by TRAD infection in a dose-dependent fashion (Fig. 1). Because H1299 cells can be obtained from ATCC, they can be used in clinical laboratories to assess the biological activity of TRAD with a qualified standard protocol. In addition, although adenoviral E1B-55 kDa protein is known to bind to the tumor suppressor p53 protein,[12] H1299 cells are p53-null and therefore the interaction of E1B-55 kDa with p53, which in turn results in transcriptional modulation, can be ignored in this cell line. Thus, H1299 is considered an appropriate cell line for assessment of TRAD activity in certain preparations. In the present study, we considered TRAD to be active when the viability of H1299 cells was reduced by more than 50% at 48 h after TRAD infection at an MOI of 1. Using this biological assay, we confirmed that heat treatment of aliquots of TRAD at 56°C for 5 min is sufficient to inactivate its antitumor potential (Fig. 2c). These results advocate the use of the H1299 cell-based cytotoxicity assay as a standard method for quantitative assessment of the biological activity of TRAD in virus stocks for clinical trials.

Various biological methods, such as determination of infectious units in plaque assays, have been used routinely in clinical trials to monitor viral loads in the peripheral circulation.[8] These methods are useful for evaluating safety because the viral titers directly reflect the infectivity of viruses. However, because the plaque assay consists of labor-intensive and time-consuming steps, real-time monitoring of the biodistribution of the virus might be difficult. Here we described the development of a quantitative real-time PCR assay that can accurately quantify genome copy numbers of TRAD over a large linear range. Using primers targeting TRAD-specific sequences, such as adenoviral E1A and IRES, real-time PCR could accurately detect the number of TRAD genomes in the plasma as well as in the cells (Figs 3,4). The assay showed that TRAD replicated even in NHLF, although the level was much lower than that in tumor cells. It is usually difficult to maintain the normal cells primarily isolated from human tissues such as human hepatocytes in the culture; however, commercially available NHLF could be cultured for several passages, suggesting that NHLF may have some characteristics different from primary isolated normal cells, including

telomerase activity. We also found that the number of viral genomes could be measured in genomic DNA purified from tissues of mice *in vivo* after injection of TRAD into the xenografts (Fig. 5). Although viral DNA could be detected even in normal tissues 70 days after intratumoral injection of TRAD, the absence of infectious virus as assessed by the plaque assay suggests that there are only DNA fragments in tissues. Our preliminary experiments have demonstrated that DNA could be isolated from tumors as small as 5 mm in diameter (data not shown). Therefore, the real-time PCR method with E1A and IRES primers permits rapid and quantitative detection of TRAD DNA in clinical samples.

We have shown recently the antiviral activity of cidofovir against TRAD *in vitro*. Cidofovir is an acyclic nucleoside phosphonate with potent broad-spectrum anti-DNA viral activity and has been approved for the treatment of many types of viruses, including cytomegalovirus and adenovirus.[13] Although viremia after TRAD administration is extremely rare because of the anti-adenovirus antibodies expected to be present in most patients, a real-time PCR-based pharmacokinetic assay can allow the early detection of disseminated virus, and thus its use could provide an indication for commencement of cidofovir treatment in clinical trials.

In summary, we have established a fast, reliable, and sensitive assay to assess the biological activity of TRAD *in vitro* and to detect the viral genome in the plasma as well as tissues *in vivo*. A phase I clinical trial of TRAD targeting advanced solid tumors is currently underway in the USA following the approval of the Food and Drug Administration. Such an assay has been used in this ongoing trial and the data will be analyzed in the near future for the assessment of the safety, efficacy, and biodistribution of TRAD.

Acknowledgments

This work was supported in part by grants from the Ministry of Education, Science, and Culture, Japan, and by grants from the Ministry of Health and Welfare, Japan.

References

1 Kohn EC, Lu Y, Wang H *et al.* Molecular therapeutics: promise and challenges. *Semin Oncol* 2004; **31**: 39–53.
2 Hawkins LK, Lemoine NR, Kirn D. Oncolytic biotherapy: a novel therapeutic platform. *Lancet Oncol* 2002; **3**: 17–26.
3 Chiocca EA. Oncolytic viruses. *Nat Rev Cancer* 2002; **2**: 938–50.
4 Reid T, Galanis E, Abbruzzese J *et al.* Hepatic arterial infusion of a replication-selective oncolytic adenovirus (dl1520): phase II viral, immunologic, and clinical endpoints. *Cancer Res* 2002; **62**: 6070–9.
5 Hamid O, Varterasian ML, Wadler S *et al.* Phase II trial of intravenous CI-1042 in patients with metastatic colorectal cancer. *J Clin Oncol* 2003; **21**: 1498–504.
6 Kawashima T, Kagawa S, Kobayashi N *et al.* Telomerase-specific replication-selective virotherapy for human cancer. *Clin Cancer Res* 2004; **10**: 285–92.
7 Kim NW, Piatyszek MA, Prowse KR *et al.* Specific association of human telomerase activity with immortal cells and cancer. *Science* 1994; **266**: 2011–15.
8 Fujiwara T, Tanaka N, Kanazawa S *et al.* Multicenter phase I study of repeated intratumoral delivery of adenoviral p53 in patients with advanced non-small-cell lung cancer. *J Clin Oncol* 2006; **24**: 1689–99.
9 Umeoka T, Kawashima T, Kagawa S *et al.* Visualization of intrathoracically disseminated solid tumors in mice with optical imaging by telomerase-specific amplification of a transferred green fluorescent protein gene. *Cancer Res* 2004; **64**: 6259–65.
10 Taki M, Kagawa S, Nishizaki M *et al.* Enhanced oncolysis by a tropism-modified telomerase-specific replication-selective adenoviral agent OBP-405 ('Telomelysin-RGD'). *Oncogene* 2005; **24**: 3130–40.
11 Watanabe T, Hioki M, Fujiwara T *et al.* Histone deacetylase inhibitor FR901228 enhances the antitumor effect of telomerase-specific replication-selective adenoviral agent TRAD in human lung cancer cells. *Exp Cell Res* 2006; **312**: 256–65.
12 Cathomen T, Weitzman MD. A functional complex of adenovirus proteins E1B-55kDa and E4orf6 is necessary to modulate the expression level of p53 but not its transcriptional activity. *J Virol* 2000; **74**: 11 407–12.
13 Ouchi M, Kawamura H, Nagai K, Urata Y, Fujiwara T. Antiviral activity of cidofovir against telomerase-specific replication-competent adenovirus, Telomelysin (OBP-301). *Mol Ther* 2007; **15** (Suppl 1): S173.

doi: 10.1111/j.1349-7006.2007.00665.x

Telomerase-Specific Oncolytic Virotherapy for Human Cancer with the hTERT Promoter

Toshiyoshi Fujiwara[1,2,*], Yasuo Urata[3] and Noriaki Tanaka[2]

[1]*Center for Gene and Cell Therapy, Okayama University Hospital, Okayama 700-8558, Japan;* [2]*Division of Surgical Oncology, Department of Surgery, Okayama University Graduate School of Medicine, Dentistry and Pharmaceutical Sciences, Okayama 700-8558, Japan;* [3]*Oncolys BioPharma, Inc., Tokyo 106-0032, Japan*

Abstract: Replication-selective tumor-specific viruses present a novel approach for treatment of neoplastic disease. These vectors are designed to induce virus-mediated lysis of tumor cells after selective viral propagation within the tumor. For targeting cancer cells, there is a need for tissue- or cell-specific promoters that can express in diverse tumor types and are silent in normal cells. Recent advances in molecular biology have fostered remarkable insights into the molecular basis of neoplasm. Telomerase activation is considered to be a critical step in carcinogenesis and its activity correlates closely with human telomerase reverse transcriptase (hTERT) expression. Since only tumor cells that express telomerase activity would activate this promoter, the hTERT proximal promoter allows for preferential expression of viral genes in tumor cells, leading to selective viral replication. We constructed an attenuated adenovirus 5 vector (Telomelysin, OBP-301), in which the hTERT promoter element drives expression of E1A and E1B genes linked with an internal ribosome entry site (IRES). Telomelysin replicated efficiently and induced marked cell killing in a panel of human cancer cell lines, whereas replication as well as cytotoxicity was highly attenuated in normal human cells lacking telomerase activity. Thus, the hTERT promoter confers competence for selective replication of Telomelysin in human cancer cells, an outcome that has important implications for the treatment of human cancers. This article reviews recent findings in this rapidly evolving field: cancer therapeutic and cancer diagnostic approaches using the hTERT promoter.

Keywords: Telomerase, hTERT, adenovirus, GFP, imaging.

INTRODUCTION

Human chromosomal end structures, named telomeres, serve as protective caps and consist of short tandemly repeated TTAGGG sequence [1, 2]. Telomere attrition contributes to genomic instability and may thereby promote the development of malignant cell transformation [3]. A fundamental difference in the behavior of normal versus tumor cells is that normal cells divide for a limited number of times, while tumor cells have the ability to proliferate indefinitely [4-6]. Telomere shortening sets a physical limit to the potential number of cell divisions and serves as a mitotic clock defining the lifespan of somatic cells [7]. One mechanism to escape this limitation is the activation or upregulation of telomerase. As telomerase can reset the mitotic clock, it has been linked to the processes of tumorigenesis and aging. Telomerase is a ribonucleoprotein complex responsible for adding TTAGGG repeats onto the 3' ends of chromosomes [8-10]. Many studies have demonstrated that the majority of malignant tumors express telomerase activity, a feature that accounts for their proliferative capacity [11-13], whereas telomerase is strongly repressed in most normal somatic tissues [14]. Therefore, telomerase has attracted considerable attention as a plausible target for cancer diagnosis and therapy [15].

The human telomerase complex is composed of three components: the RNA subunit (known as hTR, hTER, or hTERC) [16], the telomerase-associated protein (hTEP1) [17], and the catalytic subunit (hTERT, human telomerase reverse transcriptase) [18, 19]. Both hTR and hTERT are required for the reconstitution of telomerase activity *in vitro* [20] and, therefore, represent the minimal catalytic core of telomerase in humans [21]. However, while hTR is widely expressed in embryonic and somatic tissue, hTERT is tightly regulated and is not detectable in most somatic cells. The cloning of the promoter region of hTERT in 1999 [22-25] facilitated the development of targeted cancer gene therapy approaches that can specifically and markedly augment transgene expression in tumor with its specificity. Telomerase-specific expression of cytotoxic or proapoptotic genes such as the diphtheria toxin A-chain, FADD, caspases, Bax, and PUMA by the hTERT promoter has been successfully achieved and reported in various gene transfer systems (e.g., plasmid and adenovirus) [26-31]. Although adenovirus-mediated Bax gene expression via the hTERT promoter elicits a therapeutic effect on tumor cells and could prevent the toxic effects on normal cells [30], the viral spread might be less than ideal after intratumoral administration.

Replication-defective, E1-deleted adenoviral vectors facilitate the efficient delivery of a variety of transgenes to target tissues and have demonstrated clear therapeutic benefits and safety in a variety of clinical studies [32-34]; a significant obstacle, however, is the limited distribution of the vectors within the tumor mass even after direct intratumoral administration. To confer specificity of infection and increase viral spread to neighboring tumor cells, the notion of using replication-competent adenoviruses has become a reality [35-37]. The fact that activation of hTERT gene expression is one of the key events during tumorigenesis [38, 39] enables the hTERT promoter to take place in the tumor-specific transcriptional control of genes essential for viral replication. We hypothesized that an adenovirus containing the hTERT promoter-driven E1 genes could be used to target a variety of tumor cells and kill them efficiently by viral replication. Moreover, this virus can be useful for cancer diagnostics, especially for detection of minute metastases *in vivo*, since more than 85% of human cancers display telomerase activity [12].

*Address correspondence to this author at the Center for Gene and Cell Therapy, Okayama University Hospital, 2-5-1 Shikata-cho, Okayama 700-8558, Japan; Tel: 81-86-235-7997; Fax: 81-86-235-7884; E-mail: toshi_f@md.okayama-u.ac.jp

1568-0096/07 $50.00+.00

TELOMERASE AND CANCER

Telomerase Activation in Human Cancer

Cancer is characterized by unregulated proliferation of a certain cell population, which eventually affects normal cellular function in the human body [4-6]. To selectively target cancer cells, it is essential to identify the crucial molecular determinants involved in tumor progression. Cellular immortality is a critical step in tumorigenesis and, therefore, the molecular mechanism of the unlimited replicative capacity of tumor cells may provide universal and effective means for treating human cancer [15].

Telomeres are situated at the ends of linear chromosomes and protect them from degradation and end-to-end fusions [2]. Tumor cells can maintain telomere length predominantly due to the enzyme telomerase [8-10]. Telomerase activity is detected in about 85% of malignant tumors [12], whereas in most normal somatic tissues telomerase is absent [14]. Although weak telomerase activity is detected in peripheral blood leukocytes and in certain stem cell population [40, 41], the majority of malignant tumors express high levels of telomerase activity [11-13]. There is also a gradient increase in telomerase activity between early and late stage tumors. The strong association between telomerase activity and malignant tissue suggests that telomerase can be an essential target for the diagnosis and treatment of cancer.

The transcriptional upregulation of hTERT, a catalytic subunit of telomerase, represents the rate-limiting step in telomerase expression [18, 19], although other pathways involved in the control telomerase activity such as differential splicing of the hTERT transcript and posttranscriptional modification of the hTERT protein may exist [42]. Thus, the hTERT promoter region can be used as a fine-tuning molecular switch that works exclusively in tumor cells.

Regulation of hTERT Transcription

Recent studies have provided mechanistic insight into how the hTERT promoter can be stimulated or suppressed by oncogenic activation as well as inactivation of tumor suppressors. Various laboratories have identified transcription factors that are involved in upregulation or downregulation of hTERT transcriptional activity (Fig. **1**). These reports proposed a variety of potential mechanisms of the transcriptional control of hTERT, which may help us design telomerase- or hTERT-based cancer therapies.

The hTERT promoter contains two E-boxes (CACGTG) that are binding sites for the Myc/Max/Mad network of transcriptional factors [22, 24, 43, 44]. The oncoprotein c-Myc forms a complex with the Max protein that binds as a heterodimer to activate hTERT transcription. In contrast, heterodimers with Mad1 and Max proteins result in repression of hTERT expression [45, 46]. The relative levels of c-Myc and Mad1 correlate directly with activation and repression of hTERT expression. The transcriptional factor Sp1 has been reported to cooperate with c-Myc to induce the hTERT promoter, depending on cell type, suggesting a reliance on Sp1 for full activity of c-Myc [47]. Other transcriptional factors such as ETS proteins and viral proteins also contribute to hTERT upregulation. Since epidermal growth factor (EGF) receptor and its homolog, the HER2/Neu proto-oncoprotein, stimulate phosphorylation of MAP kinases [48], which in turn activate ETS1/ETS2 [49], stimulation by EGF can lead to hTERT upregulation. The human papilloma virus (HPV) type 16 E6 protein can also associate with c-Myc and thereby activate the hTERT promoter [50-52].

In addition to Mad1, several dominant repressors that mediate hTERT downregulation have been identified. For example, the Wilm's tumor suppressor 1 (WT1) and myeloid-specific zinc finger protein 2 (MZF-2) interact with the hTERT promoter, to suppress hTERT transcription [53, 54]. Based on the preferential expression of WT1 in kidney, gonads, and spleen and of that of MZF-2 in myeloid cells, WT1 and MZF-2-mediated repression of hTERT seems tissue-specific. Other transcriptional factors, E2F-1, E2F-2, and E2F-3, also repress hTERT transcription by binding to the hTERT promoter [55, 56].

The hTERT transcription is also regulated by nuclear hormones as well as drugs that involve gene expression. Estrogen induces an increase in hTERT mRNA levels through the estrogen receptor (ER), which interacts with two estrogen response elements (EREs) in the hTERT promoter [57, 58]. Progesterone and androgen also stimulate telomerase activity through hTERT expression, although this response is likely to be indirect [59]. Furthermore, histone deacetylase (HDAC) inhibitors activate the transcription of certain genes by altering the acetylation status of nucleosomal histones. It has been reported that treatment with HDAC inhibitor, tricostatin A (TSA), could induce significant activation of hTERT mRNA

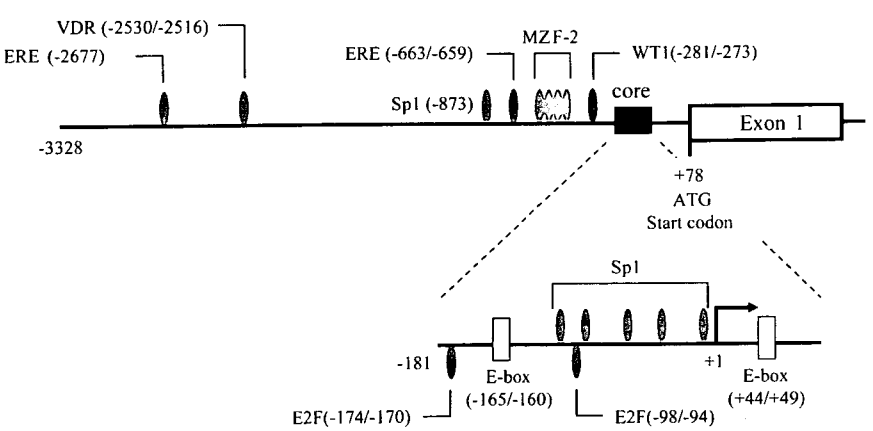

Fig. (1). Scheme of the proximal promoter of hTERT. Putative protein binding sites for various transcription factors are indicated.

expression and telomerase activity in normal cells through the TSA-responsive element localized in the hTERT proximal promoter [60]. In contrast, nonsteroidal anti-inflammatory drugs (NSAIDs) such as aspirin, indomethacin, and cyclooxygenase (COX)-2 inhibitor have been recently shown to inhibit telomerase activity at the hTERT transcriptional level in colon cancer cells [61]. The *cis*-response elements to NSAIDs have been identified in the hTERT promoter region. Furthermore, some nuclear hormone receptors including vitamin D receptor and retinoic acid receptor can repress hTERT expression [62, 63].

These observations gained from the study of hTERT transcriptional regulation suggest that hTERT activity in cancer cells can be modified by exogenous stimuli such as hormones, drugs, and genes, which may enhance the anti-tumor effects of hTERT-specific cancer therapies as combined modalities.

hTERT PROMOTER FOR CANCER THERAPEUTICS

Construction of Telomelysin

The use of modified adenoviruses that replicate and complete their lytic cycle preferentially in cancer cells is a promising strategy for treatment of cancer. One approach to achieve tumor specificity of viral replication is based on the transcriptional control of genes that are critical for virus replication such as E1A or E4. For example, the heterologous promoters from the prostate-specific antigen (PSA) [64], MUC1 [65], osteocalcin [66], L-plastin [67], midkine [68], and E2F-1 [69] genes have been used to drive E1A expression. These vectors replicate preferentially in tumor cells that express each targeted tumor marker; their therapeutic window, however, is relatively narrow because only part of the tumor is positive for each tumor marker. As described above, telomerase, especially its catalytic subunit hTERT, is expressed in the majority of human cancers and the hTERT promoter is preferentially activated in human cancer cells [12]. Thus, the broadly applicable hTERT promoter might be a suitable regulator of adenoviral replication. Indeed, it has been reported previously that the transcriptional control of E1A expression via the hTERT promoter could restrict adenoviral replication to telomerase-positive tumor cells and efficiently lyse tumor cells [70-72].

The adenovirus E1B gene is expressed early in viral infection and its gene product inhibits E1A-induced p53-dependent apoptosis, which in turn promote the cytoplasmic accumulation of late viral mRNA, leading to a shut down of host cell protein synthesis. In most vectors that replicate under the transcriptional control of the E1A gene including hTERT-specific oncolytic adenoviruses, the E1B gene is driven by the endogenous adenovirus E1B promoter. However, Li *et al.* have demonstrated that transcriptional control of both E1A and E1B genes by the α- fetoprotein (AFP) promoter with the use of IRES significantly improved the specificity and the therapeutic index in hepatocellular carcinoma cells [73]. Therefore, we have developed Telomelysin (OBP-301), in which the tumor-specific hTERT promoter regulates both the E1A and E1B genes (Fig. **2**). Telomelysin controls the viral replication more stringently, thereby providing profound therapeutic effects in tumor cells as well as the attenuated toxicity in normal tissues [74].

The construction of Telomelysin was carried out as follows. An 897-bp fragment of the E1A gene and a 1822-bp fragment of the E1B gene were amplified by PCR from cellular RNA and genomic DNA of 293 cells, respectively. The amplified products were subcloned into the pTA plasmid. Following confirmation by DNA nucleotide sequencing, the E1A (911 bp) and E1B (1836 bp) genes were cloned into the pIRES vector (pE1A-IRES-E1B). A 455-bp fragment of the hTERT promoter, which contains a 378-bp region upstream of the transcription start site, was ligated into the pE1A-IRES-E1B (phTERT-E1A-IRES-E1B). The 3828-bp fragment was digested from the phTERT-E1A-IRES-E1B and then cloned into pShuttle after deletion of the cytomegalovirus (CMV) promoter. The resultant shuttle vector was applied to the Adeno-X Expression System (Clontech Laboratories, Palo Alto, CA). Recombinant adenovirus was isolated from a single plaque and expanded in 293A cells. The resultant virus was termed Telomelysin.

The 181-bp fragment upstream of the transcription start site is considered the core functional promoter that is essential for transcriptional activation of hTERT in tumor cells. Takakura *et al.* reported by analysis of 5'-truncations of the promoter that hTERT transcriptional activity decreased with deletion of sequences between -776 and -1375 and increased with the deletion of sequences between -378 and -776, indicating that *cis*-acting and silencer elements, respectively, exist in these regions [22]. They also demonstrated that the 378-bp fragment that we used for Telomelysin could exhibit high transcriptional activity similar to that of the 181-bp core promoter region.

Functional Analysis of Telomelysin

Methods used for measuring viral replication of Telomelysin include standard plaque assay using 293 cells as well as quantitative real-time PCR analysis targeting for the viral E1A or IRES sequence [74, 75], both of which present similar replication patterns of Telomelysin in human cancer cells. Telomelysin induced selective E1A and E1B expression in cancer cells, which resulted in viral replication at 5-6 logs by 3 days after infection; Telomelysin replication, however, was attenuated up to 2 logs in cultured normal cells [74, 75]. Although the transduction efficiency of adenovirus is less efficient in normal cells compared with tumor cells, the observation that wild-type adenovirus infection killed normal cultured cells more effectively suggests that the attenuated cytotoxicity of Telomelysin in normal cells is due to tumor-specific replication, but not due to the low transduction. These data indicate that selective replication of Telomelysin is both therapeutically beneficial and safe. The relative E1A DNA levels determined by quantitative real-time PCR assay after Telomelysin infection correlated with hTERT mRNA expression levels in several human cancer cell lines, suggesting that Telomelysin viral yields are closely associated with the hTERT transcriptional activity in human cancer.

The majority of human cancer cells acquire immortality and unregulated proliferation by expression of the hTERT [12] and, therefore theoretically, hTERT-specific Telomelysin can possess a broad-spectrum antineoplastic activity against a variety of human tumors. *In vitro* cytotoxicity assays demonstrated that Telomelysin could efficiently kill various types of human cancer cell lines including head and neck cancer, lung cancer, esophageal cancer, gastric cancer, colorectal cancer, breast cancer, pancreatic cancer, hepatic cancer, prostate cancer, cervical cancer, melanoma, sarcoma, and mesothelioma in a dose-dependent manner. The dose of Telomelysin that causes